

Depth of the Martian cryosphere: Revised estimates and implications for the existence and detection of subpermafrost groundwater

Stephen M. Clifford, Jeremie Lasue, Essam Heggy, Joséphine Boisson, Patrick Mcgovern, Michael D. Max

▶ **To cite this version:**

Stephen M. Clifford, Jeremie Lasue, Essam Heggy, Joséphine Boisson, Patrick Mcgovern, et al.. Depth of the Martian cryosphere: Revised estimates and implications for the existence and detection of subpermafrost groundwater. Journal of Geophysical Research. Planets, 2010, 115, 10.1029/2009JE003462 . insu-03605310

HAL Id: insu-03605310
https://insu.hal.science/insu-03605310

Submitted on 11 Mar 2022

HAL is a multi-disciplinary open access archive for the deposit and dissemination of scientific research documents, whether they are published or not. The documents may come from teaching and research institutions in France or abroad, or from public or private research centers.

L'archive ouverte pluridisciplinaire **HAL**, est destinée au dépôt et à la diffusion de documents scientifiques de niveau recherche, publiés ou non, émanant des établissements d'enseignement et de recherche français ou étrangers, des laboratoires publics ou privés.

Copyright

JOURNAL OF GEOPHYSICAL RESEARCH, VOL. 115, E07001, doi:10.1029/2009JE003462, 2010

Click Here for Full Article

Depth of the Martian cryosphere: Revised estimates and implications for the existence and detection of subpermafrost groundwater

Stephen M. Clifford,[1] Jeremie Lasue,[1] Essam Heggy,[2] Joséphine Boisson,[2] Patrick McGovern,[1] and Michael D. Max[3]

Received 1 July 2009; revised 5 October 2009; accepted 23 December 2009; published 2 July 2010.

[1] The Martian cryosphere is defined as that region of the crust where the temperature remains continuously below the freezing point of water. Previous estimates of its present thickness have ranged from ~2.3–4.7 km at the equator to ~6.5–12.5 km at the poles. Here we revisit these calculations, review some of the assumptions on which they were based, and investigate the effects of several parameters, not previously considered, on the cryosphere's thermal evolution and extent. These include astronomically driven climate change, the temperature-dependent thermal properties of an ice-rich crust, the potential presence of gas hydrate and perchlorate-saturated groundwater, and consideration of recent lower estimates of present-day global heat flow (which suggest a mean value roughly half that previously thought, effectively doubling the potential thickness of frozen ground). The implications of these findings for the continued survival of subpermafrost groundwater and its potential detection by the MARSIS radar sounder onboard Mars Express are then discussed. Although our estimates of the maximum potential thickness of the cryosphere have significantly increased, consideration of the likely range and spatial variability of crustal heat flow and thermal properties, in combination with the potential presence of potent freezing point depressing salts, may result in substantial local variations in cryosphere thickness. The locations that appear best suited for the detection of groundwater are those that combine low latitude (minimizing the thickness of frozen ground) and low elevation (minimizing the depth to a water table in hydrostatic equilibrium). Preliminary results from a MARSIS investigation of one such area are discussed.

Citation: Clifford, S. M., J. Lasue, E. Heggy, J. Boisson, P. McGovern, and M. D. Max (2010), Depth of the Martian cryosphere: Revised estimates and implications for the existence and detection of subpermafrost groundwater, *J. Geophys. Res.*, *115*, E07001, doi:10.1029/2009JE003462.

1. Introduction

[2] Consideration of the volume of water required to erode the Martian outflow channels, and the likely subsurface extent of their original source regions, suggests that at the time of their formation, Mars possessed a planetary inventory of water equal to a global equivalent layer (GEL) ~0.5–1 km deep [*Carr*, 1986, 1996] Because the time of peak outflow channel activity (~3 Ga [*Tanaka*, 1986; *Hartmann and Neukum*, 2001]) postdates the period when the most efficient mechanisms of water loss (hydrodynamic escape and atmospheric erosion by large impacts) were thought to be active (>4 Ga [*Melosh and Vickery*, 1989; *Carr*, 1999]), it is expected that the bulk of water from this era still persists today, although, since the Late Hesperian, ~15 m may have been lost to space [*Valeille et al.*, 2010], an unkown quantity was consumed by the formation of hydrated minerals, and ~5 m appears to have been added to planetary inventory by the exsolution of H_2O from Martian magmas [*Craddock and Greeley*, 2009].

[3] Of the inventory of water that remains today, nearly all (~90–95% [*Carr*, 1986, 1996]) is now believed to reside in two thermally distinct subsurface reservoirs: as ground ice, within the near-surface region of perennially frozen ground (known as the cryosphere), and as groundwater, located deeper in the crust, where radiogenic heating is expected to have increased lithospheric temperatures above the freezing point (Figure 1 [*Fanale*, 1976; *Rossbacher and Judson*, 1981; *Kuzmin*, 1983; *Carr*, 1996; *Clifford*, 1993; *Clifford and Parker*, 2001]).

[1]Lunar and Planetary Institute, Houston, Texas, USA.
[2]Equipe Géophysique Spatiale et Planétaire, Institut de Physique du Globe de Paris, Université Paris Diderot, CNRS, St Maur des Fosses, France.
[3]MDS Research, St. Petersburg, Florida, USA.

Copyright 2010 by the American Geophysical Union.
0148-0227/10/2009JE003462

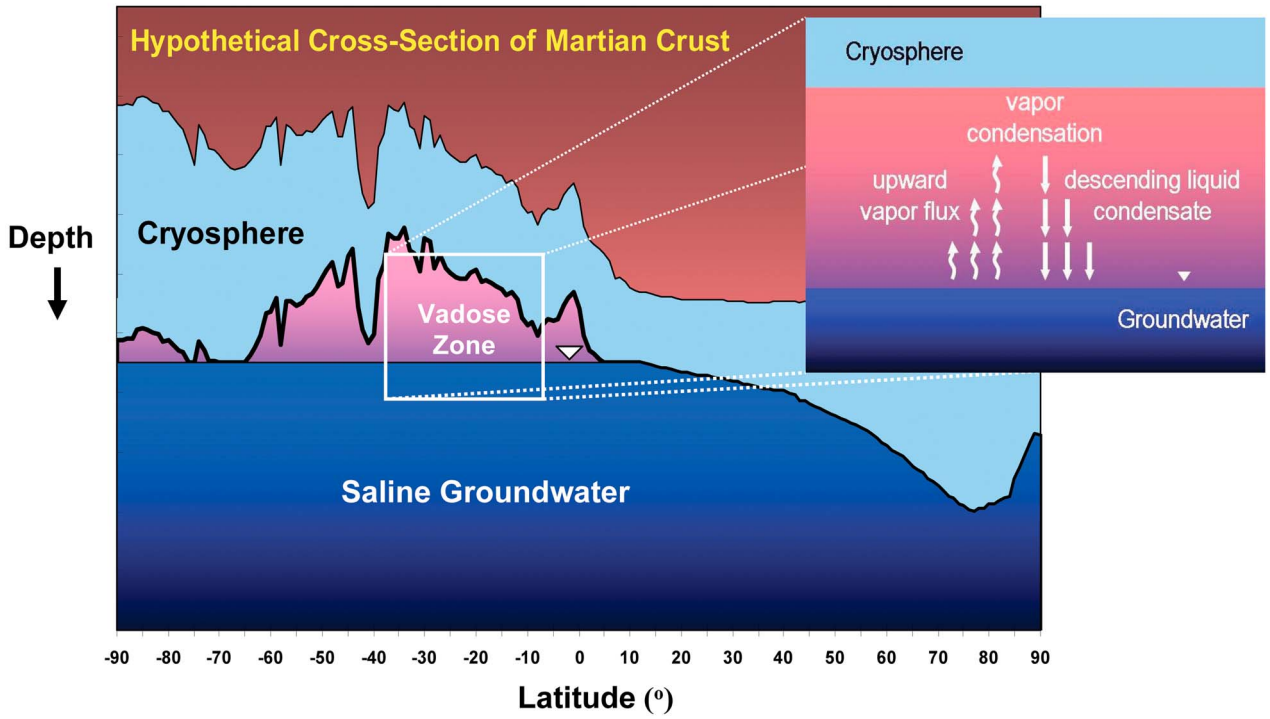


Figure 1. A hypothetical pole-to-pole cross section of the present-day Martian crust (along 203°E longitude), illustrating the potential relationship between surface topography, ground ice, and groundwater. Surface elevations are from the MOLA Mission Experiment Gridded Data Record with a 2° smoothing function [*Smith et al.*, 2003]. At those locations where the base of the cryosphere is in contact with the water table, the presence of dissolved salts may reduce the thickness of frozen ground by depressing the freezing point of the groundwater to a value as low as the 203 K eutectic temperature of a saturated $Mg(ClO_4)_2$ brine. Conversely, where the cryosphere and groundwater are not in direct contact, the leaching of soluble salts by low-temperature hydrothermal convection (see inset and discussion from *Clifford* [1993]) may result in basal melting temperatures closer to ~273 K. Note that local variations in the thermal, diffusive, and hydraulic properties of the crust are likely to result in significant differences in the distribution of ground ice and groundwater from that depicted here. After Figure 1 of *Clifford and Parker* [2001].

[4] Because the cryosphere is a natural cold trap for subsurface water, the fraction of the subsurface inventory that persists as groundwater depends on the relative size of that inventory with respect to the accessible pore volume of the cryosphere [*Clifford*, 1993]. If this inventory exceeds the pore volume of the cryosphere, then the excess H_2O will be stored as groundwater, saturating the lowermost porous regions of the crust. On the other hand, if the subsurface inventory of H_2O is less than the pore volume of the cryosphere, then all of the planet's original inventory of water may now be cold trapped within the cryosphere, except where groundwater may be transiently produced by thermal disturbances of the crust, such as impacts, volcanism and climate change.

[5] The extent of the cryosphere, and the continued survival of groundwater at depth, have important implications for understanding the hydrological and mineralogical evolution of the Martian crust, as well as the potential survival of life in deep subsurface habitats, where it would have been isolated from the effects of oxidants, climate change and large, surface-sterilizing impacts [*Onstott et al.*, 2006].

[6] Based on previous best estimates of mean global heat flow, the thermal properties of the crust, and the current range of mean annual surface temperatures, *Clifford* [1993] estimated that the nominal depth of the cryosphere varied from ~2.3 km at the equator to ~6.5 km at the poles, noting the potential for significant (±50%) local variations due to the likely heterogeneity of crustal heat flow and thermal properties. Taking into account the temperature dependence of the thermal conductivity of rock and water ice, *Clifford and Parker* [2001] estimated a slightly greater range of nominal thicknesses, ~2.5–4.7 km at the equator and ~6.5–12.5 km at the poles, again, with the expectation of significant local variability.

[7] Here we revisit these calculations, examining the potential consequences and implications of our evolving understanding of crustal thermal conductivity (including the effects of lithology, desiccation and gas hydrates), astronomically induced variations in mean annual surface temperature, the potential occurrence of potent freezing point depressing salts (such as perchlorate), the effects of hydrothermal circulation, and recent lower estimates of present-day global heat flow. We conclude that the present Martian

cryosphere may be up to twice as deep as previously thought and discuss the potential implications for the hydrologic and mineralogic evolution of the crust, the continued survival of subpermafrost groundwater, and the potential detectability of deep groundwater by the MARSIS orbital radar sounder onboard the European Space Agency's (ESA) Mars Express spacecraft.

2. Revised Estimates of the Depth of the Cryosphere

[8] The Martian cryosphere is defined as the region of frozen ground extending from the surface down to a local depth, z, given by the solution to the one-dimensional heat conduction equation

$$z = k_{(T)} \frac{(T_{mp} - T_{ms})}{Q_g}, \quad (1)$$

where $k_{(T)}$ is the temperature-dependent thermal conductivity of the crust, T_{ms} is the latitudinaly variable mean surface temperature, T_{mp} is the melting temperature of ice at the base of the cryosphere (which can be depressed below 273 K by the effects of pressure and freezing point depressing salts), and Q_g is the geothermal heat flux [*Clifford*, 1993; *Clifford and Parker*, 2001]. In the following discussion, we review previous estimates of these parameters, as well as the improvements and revisions made in the current analysis.

2.1. Thermal Conductivity

[9] Based on a synthesis of 445 laboratory measurements of the thermal conductivity of frozen soil and basalt, *Clifford* [1993] concluded that the column-averaged thermal conductivity of the Martian cryosphere had a probable mean value of ~2 W m^{-1} K^{-1} (±1 W m^{-1} K^{-1}). However, many of these measurements were made at temperatures between 253–273 K, where the presence of thin films of unfrozen water on soil particle surfaces would have contributed to lower thermal conductivities than expected under the much colder temperature conditions generally found on Mars.

[10] Beyond the effect of unfrozen water, the thermal conductivity of both rock and water ice are temperature dependent. Although few measurements of the thermal conductivity of basalt have been made at temperatures < 273 K, its thermal conductivity above 273K increases with decreasing temperature [*Clauser and Huenges*, 1995; *Lee and Deming*, 1998]. Given the range of thermal conductivities characteristic of dense basalt at room temperature (cf., values summarized in Table 2 of *Clifford* [1993]) and an extrapolation of basalt's observed temperature dependence to subfreezing temperatures, suggests that the thermal conductivity of dense basalt is generally equal to or greater than that of water ice at equivalent temperatures, i.e.,

$$k_{(T)} = \frac{488.19}{T} + 0.4685, \quad (2)$$

which varies from a low of 2.26 W m^{-1} K^{-1} at 273 K, to a high of 3.64 W m^{-1} K^{-1} at 154 K [*Hobbs*, 1974].

[11] One important caveat to this higher estimate of effective crustal thermal conductivity is the possibility that methane hydrate (rather than water ice) is the principal volatile component of the cryosphere. This possibility is suggested by the apparent subsurface origin of the methane recently detected in the Martian atmosphere [*Formisano et al.*, 2004; *Krasnopolsky et al.*, 2004; *Mumma et al.*, 2004, 2009]. Various studies suggest that large quantities of methane may have been produced, either biotically or abiotically, within the subsurface, where it may have become trapped, under conditions of low temperature and high pressure, within the crystalline lattice of water ice, forming methane hydrate [*Kargel and Lunine*, 1998; *Fisk and Giovannoni*, 1999; *Max and Clifford*, 2000].

[12] In its pure state, the thermal conductivity of gas hydrate is ~0.5 W m^{-1} K^{-1} [*Davidson*, 1983; *Sloan*, 1997], or approximately one-fifth that of water ice at 273 K, a value that recent laboratory measurements have demonstrated remains fairly constant over a broad range of subfreezing temperatures [*Krivchikov et al.*, 2005]. Thus, depending on the cryospheric abundance and distribution of gas hydrate, it may contribute to a significant reduction in the effective thermal conductivity of the crust, especially at shallow depths (within the top ~km), where the porosity of the crust is expected to be the highest (~20–35%, see section 2.5).

[13] Finally, at latitudes ≤ 40°, ground ice is unstable with respect to the water vapor content of the atmosphere, leading to the progressive desiccation of the regolith [*Clifford and Hillel*, 1983; *Fanale et al.*, 1986; *Mellon and Jakosky*, 1993]. The rate and ultimate extent of local desiccation is dependent on the mean annual surface temperature, as well as the local thermal and diffusive properties of the crust. Depending on the nature of these properties, their variation with depth, and the potential for replenishment from any deeper reservoir of crustal water, these factors may result in local depths of desiccation that range from several meters to as much as a kilometer or more beneath the surface [*Clifford*, 1993, 1998; *Mellon et al.*, 1997]. The effective thermal conductivity of an ice-free fine-grained sedimentary regolith, with a typical thermal inertia of 220 J m^{-2} K^{-1} s$^{-1/2}$, is ~0.06 W m^{-1} K^{-1} [*Presley and Christensen*, 1997], a value that can vary by more than an order of magnitude depending on the regolith particle size and the degree of consolidation.

2.2. Surface Temperature

[14] Current mean annual surface temperatures on Mars range from ~218 K at the equator to ~154 K at the poles, with local variations of up to ±5 K at any latitude due to geographical variations in albedo and thermal inertia [*Clifford*, 1993]. However, because the obliquity and orbital elements of Mars vary with time, so too does the mean annual insolation and temperature at any given latitude.

[15] The obliquity of Mars (which is currently 25.2°) varies with a period of ~1.2 × 10^5 yrs, with maximum-to-minimum fluctuations of as much as 20–30°. The amplitude of this oscillation is also modulated with a period of 1.3 × 10^6 years [*Ward*, 1992] and varies chaotically on a timescale of ≥10^7 years, with extreme values ranging from 0° to over 60° [*Laskar and Robutel*, 1993; *Touma and Wisdom*, 1993; *Laskar et al.*, 2004]. Other astronomical variables include the 5.1 × 10^4 year precessional cycle and two superposed periods of change in orbital eccentricity, a 9.5 × 10^4 year

cycle with a peak-to-peak amplitude of 0.04, and a 2×10^6 year cycle with an amplitude of 0.1 [*Ward*, 1992].

[16] The mean annual insolation, $S(l)$, at any latitude l and obliquity i, is given by the expression

$$\overline{S}(l) = \frac{1}{2\pi^2} \frac{S_0}{\sqrt{1-e^2}} \int_0^{2\pi} \sqrt{1-(\sin l \cos i - \cos l \sin i \sin \psi)^2}\, d\psi, \tag{3}$$

where S_0 is the solar constant at the orbit's semimajor axis, e is the orbital eccentricity, and. ψ is an integration variable [*Ward*, 1974; *Schorghofer*, 2008]. From this mean insolation, a corresponding mean annual surface temperature can be calculated based on the assumption of radiative equilibrium, i.e.,

$$T_m(l) \approx \left[1.05 \times \frac{(1-A)S(l)}{\varepsilon\sigma}\right]^{1/4}, \tag{4}$$

where $T_m(l)$ is the mean annual temperature at a latitude l, A is the albedo, ε is the emissivity, σ is the Stefan-Boltzmann constant, and the numerical coefficient "1.05" reflects the 5% increase in mean annual radiation from the atmosphere, relative to the mean annual insolation at the surface.

[17] Mean annual temperatures that are calculated using this approach are generally accurate at latitudes below ~45° and at latitudes above the perimeter of the perennial polar caps (~80°–85°). However, at those latitudes that lie in between, equation (4) yields mean annual temperatures that consistently exceed observed Martian values. This is due to the fact that above ~45°, part of the mean annual insolation is reflected back into space due to the formation of the seasonal polar caps. Therefore, to accurately reproduce the observed range of Martian mean annual surface temperatures requires numerical simulations of diurnal and seasonal temperature variations that include not only the effects of insolation and radiation, but the condensation and sublimation of atmospheric CO_2.

2.3. Freezing Point Depression

[18] The freezing point of Martian groundwater can be significantly depressed by the presence of dissolved salts [*Clark*, 1978; *Brass*, 1980; *Clark and Van Hart*, 1981; *Burt and Knauth*, 2003; *Fairén et al.*, 2009]. The evolution of Martian groundwater into a highly mineralized brine is an expected consequence of three processes: (1) the leaching that occurs when groundwater is in direct contact with crustal rocks, (2) the increased concentration of dissolved minerals resulting from the depletion of groundwater in response to the growth of the cryosphere over geologic time, and (3) the influx of salts and other minerals leached from the vadose zone between the water table and base of the cryosphere by the hydrothermal circulation of water vapor and liquid condensate (inset, Figure 1) [*Clifford*, 1991, 1993].

[19] As a result, at those locations where the cryosphere is in direct contact with groundwater, the presence of dissolved salts may significantly reduce the local depth of frozen ground. Early studies of the chemical and thermodynamic stability of various salts on Mars suggested that NaCl brines (which have a freezing point of ~252 K at their eutectic) were the most likely to be found within the crust [*Clark and Van Hart*, 1981; *Burt and Knauth*, 2003], although other chloride-rich, multicomponent brines (including potential mixtures of $CaCl_2$, $MgCl_2$ and LiCl) might also exist with freezing points as low as ~210 K [*Brass*, 1980; *Clark and Van Hart*, 1981; *Burt and Knauth*, 2003].

[20] However, the stability of chloride brines is strongly influenced by the presence of sulfur, which is abundant on Mars in the form of Mg, Ca, and Fe sulfates [*Clark and Van Hart*, 1981; *Tosca and McLennanet*, 2008]. Indeed, chemical analyses of the sulfates present in the soils at Meridiani Planum (as investigated by the Mars Exploration Rover Opportunity) indicate that the composition of the local groundwater, from which local sulfates are believed to have been derived, must have had initial S/Cl ratios of ~6–30 [*Tosca and McLennanet*, 2008]. The sulfate-rich brines that are produced under these conditions depress the freezing point by only ~5 K [*Clark and Van Hart*, 1981]. Compositional variations observed within the evaporite deposits at Meridiani indicate that whether by progressive freezing or evaporation, as the original brines became more concentrated, they precipitated sulfate minerals and evolved more chloride-rich brines with lower freezing points [*Tosca and McLennanet*, 2008; *Fairén et al.*, 2009].

[21] Subpermafrost groundwater on Mars is likely to have undergone a similar evolution, with the precipitation of sulfates and carbonates, and the concentration of more Cl-rich brines, as more of the initial groundwater inventory was cold trapped into the thickening cryosphere. However, as predicted by *Clark et al.* [2005], chlorides are not the only form that Cl may take in the Martian soil.

[22] The Martian surface is highly oxidized, a likely consequence of the photochemical production of oxidants in both the atmosphere and at the surface [*Oyama and Berdahl*, 1977; *Hunten*, 1979]. One example of such a process is the reaction of volcanically derived HCl with atmospheric ozone, resulting in the production of perchlorate, which can precipitate from the atmosphere at high latitudes during the formation of the seasonal polar caps [*Catling et al.*, 2009]. Perchlorate can also be generated by the photochemical oxidation of chloride salts in the soil by solar UV [*Miller et al.*, 2006]. Evidence that Martian soils, at high latitude, contain up to 1 wt% of perchlorate, most likely in the form of $Mg(ClO_4)_2$, was provided by the investigations of the Wet Chemistry Lab (WCL) and Thermal and Evolved Gas Analyzer (TEGA) onboard the Phoenix Lander [*Hecht et al.*, 2009]. The discovery of perchlorate is significant because it is highly deliquescent, relatively inert (which allows its concentration to build up over time) and is a potent freezing point depressing salt, with its $Mg(ClO_4)_2$ form having a eutectic temperature of ~203 K [*Hecht et al.*, 2009].

[23] Although rare on Earth, perchlorate can be found in hyperarid environments like the Atacama Desert in Chile [*Ericksen*, 1981]. Its limited detection elsewhere on Earth is a likely consequence of its high solubility, which makes it easily dissolved and removed by rainfall, to ultimately mix with local surface and groundwater.

[24] In a similar way, the precipitation, infiltration and runoff of rainwater associated with a warm early greenhouse climate or large impacts [*Craddock and Maxwell*, 1993; *Craddock and Howard*, 2002; *Segura et al.*, 2002; *Mangold*

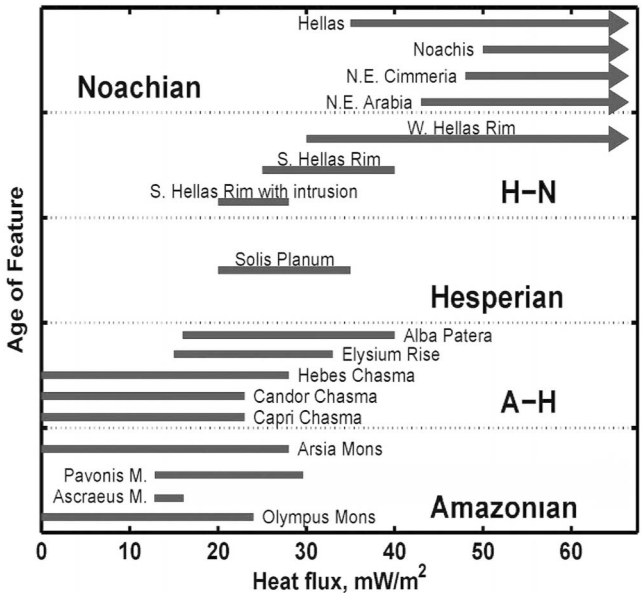


Figure 2. Regional heat flow versus time as deduced from rheologic estimates of the thickness of the elastic lithosphere. Lithospheric heat flux Q_g (in mW m^{-2}) versus surface age for several regions on Mars. The three principal age subdivisions correspond to the Noachian, Hesperian, and Amazonian epochs; while H-N and A-H identify features whose surface age appears to span two epochs. Within a given age subdivision, vertical positions give an approximate indication of the relative surface ages of features, although the development of many of these overlapped in time. Arrows indicate that Q_g has an upper bound that exceeds the values shown. Lines indicate the range of Q_g for best fit models; for all other locations with arrows, the best fit values are unbounded. After Figure 3 of *McGovern et al.* [2004].

et al., 2004] may have dissolved perchlorate and introduced it into groundwater or early Martian lakes and seas [*Hecht et al.*, 2009]. As the climate transitioned to colder conditions, the development and downward propagation of a freezing front in the crust would have inhibited further removal of perchlorate from the surface environment, although this may have had little impact on the dissolution and redistribution of perchlorate at greater depths.

[25] As discussed by *Clifford* [1991, 1993], where a vadose (unsaturated) zone exists between the base of the cryosphere and local groundwater table (as depicted in Figure 1), the presence of even a modest geothermal gradient (i.e., ~15 K km^{-1}) will give rise to the development of a low-temperature hydrothermal circulation system of ascending water vapor and descending liquid condensate within the crust. Given reasonable estimates of crustal porosity and pore size, the equivalent of a 1 km deep global ocean could have been cycled through the vadose zone planet wide by this process every ~10^6–10^7 years. An important mineralogical consequence of this activity would have been the depletion of any easily dissolved substances from the vadose zone and their concentration in the underlying groundwater, potentially up to the point of saturation and precipitation beneath the water table.

[26] This mineralogical evolution has potential consequences for the extent of the cryosphere in that where the cryosphere and saline groundwater are not in direct contact, low-temperature hydrothermal convection is likely to have depleted the intervening crust of any potent freezing point depressing salts, resulting in a cryosphere basal temperature near ~273 K, which maximizes the local depth of frozen ground. Conversely, where the cryosphere and saline groundwater are in direct contact (the likelihood of which increases at lower elevation, Figure 1), eutectic concentrations of perchlorate or other dissolved salts may dramatically thin and, in some places, potentially eliminate the local thickness of frozen ground (e.g., where the mean annual temperature exceeds the freezing point of the brine).

2.4. Heat Flow

[27] Early estimates of the present-day mean global heat flow of Mars varied between 15–45 mW m^{-2} [*Clifford*, 1993], with a nominal value of ~30 mW m^{-2}, based on the assumption that Mars possesses a chondritic composition [*Fanale*, 1976]. However, values derived from recent rheologic estimates of the thickness of the elastic lithosphere [*Solomon and Head*, 1990; *McGovern et al.*, 2004; *Plaut et al.*, 2007; *Phillips et al.*, 2008] and theoretical studies of present-day mantle convection [*Li and Kiefer*, 2007], are significantly lower (~8–25 mW m^{-2}).

[28] Although much of this evidence is specific to selected regions (as summarized by *McGovern et al.* [2004] and reproduced in Figure 2) and supported by more recent values derived from the lack of deflection observed beneath the north and south polar layered deposits (PLD) [*Plaut et al.*, 2007; *Phillips et al.*, 2008], it represents a diverse enough distribution, in both space and time, to provide important insights into the planet's long-term geothermal evolution and the most plausible range of present-day lithospheric heat flow (~15 mW m^{-2} ± 10 mW m^{-2}) estimates that are also consistent with theory [*Li and Kiefer*, 2007]. If correct, this lower estimate of present-day heat flow effectively doubles the expected thickness of frozen ground on Mars.

[29] Most previous estimates of cryosphere thickness have generally assumed that heat flow through the crust occurs only by 1-D steady state conduction (i.e., equation (1)). However, recent work by *Travis et al.* [2003] and *Travis and Feldman* [2009] has demonstrated that if groundwater is present and in contact with the base of the cryosphere (Figure 1), the assumption of steady state conduction may not always be true. Given lithospheric heat flow values ≥ 20 mW m^{-2}, permeabilities equal to (or exceeding) those estimated by *Clifford and Parker* [2001], and reasonable values of groundwater viscosity (i.e., up to those appropriate for a saturated $CaCl_2$ brine), they show that the hydrothermal convection of subpermafrost groundwater, may result in significant spatial and temporal variations in heat flow and cryosphere thickness.

[30] Although it is not clear whether conditions for the hydrothermal convection of groundwater exist on Mars today; given a mean global heat flow of ~15 mW m^{-2}, perhaps as much as ~10–30% of the planet may satisfy the necessary minimum heat flow criteria (i.e., $Q \geq 20$ mW m^{-2}), especially in areas that display relatively recent evidence of geothermal activity, such as Elysium and Tharsis. Surveys

of continental heat flow on Earth [*Pollack et al.*, 1993] indicate that on spatial scales of ~10^4–10^5 km^2, there can be a ±50% variation in local heat flow, about the global mean, due to local differences in crustal age; thickness; volcanic and tectonic history; and elemental content of U, Th and K. Over smaller horizontal distances (~10–100 km), local variations of as much as a factor of several can occur [*Blackwell*, 1971]. Given the observed geologic diversity, and our current understanding of the crustal evolution of Mars [e.g., *Nimmo and Tanaka*, 2005; *Solomon et al.*, 2005; *Watters et al.*, 2007a], it seems reasonable to expect that value of Martian heat flow will exhibit a comparable range of spatial variability.

[31] The permeability conditions necessary to sustain the hydrothermal circulation of groundwater do not appear constraining, as they lie within the range of those estimated for Mars, based on the gravitational scaling of the permeability versus depth relationship observed on the Earth [*Manning and Ingebritsen*, 1999; *Clifford and Parker*, 2001]. Like many other crustal attributes, local permeabilities are expected to exhibit significant spatial heterogeneity and cover a broad range. For example, various investigators have argued that permeabilities as high as 10^{-9} m^2 are required to support the inferred discharge rates associated with some outflow channels [*Carr*, 1979; *MacKinnon and Tanaka*, 1989; *Manga*, 2004]. While local permeabilities this high may well occur on Mars, terrestrial studies [*Brace*, 1980, 1984; *Manning and Ingebritsen*, 1999] suggest that the characteristic mean permeability of the Martian crust may be up to 4–5 orders of magnitude smaller [*Clifford* 1993].

[32] The most serious constraint on the potential contribution of hydrothermal convection to thinning the cryosphere is the extent to which groundwater and the base of the cryosphere are in physical contact, a condition that if it occurs at all on Mars, is most probable beneath regions of low elevation (Figure 1 and section 3.3). While there is no question that high-temperature vapor phase hydrothermal convection associated with active geothermal environments on Mars is also capable of transporting significant amounts of heat that could affect the local thickness of frozen ground [*Gulick*, 1998], it is unclear whether low-temperature vapor phase convection, driven solely by the planet's ambient geothermal heat flow, has that same potential.

[33] *Travis et al.* [2003] found that hydrothermal convection had little impact on the average thickness or volume of the cryosphere compared with that predicted by a 1-D thermal conduction model. This is because the principal effect of hydrothermal convection is simply to redistribute the ambient crustal heat flow, which it does through the formation of convective groundwater rolls and plumes that reduce cryosphere thickness over upwellings and increase it over downwellings, resulting in a zero net effect.

[34] Assuming a mean annual surface temperature of 213 K (representative of equatorial latitudes) *Travis et al.* [2003] found that a heat flow of 20 mW m^{-2} was sufficient to drive weak convection, but only if the permeability of the crust declined very slowly with depth. Under these conditions, the thickness of the cryosphere was reduced from an average of 6.5 km to a minimum of 5 km over plumes. Increasing the heat flow to 40 mW m^{-2}, resulted in much more vigorous convection, at lower permeabilities, and typically reduced cryosphere thickness over plumes to 1.25–2.2 km (versus a 3.9 km average over other areas). Under optimal conditions, including the assumption a 20 K higher surface temperature (233 K), the thickness of the cryosphere was reduced to as little as 300 m over narrow (0.5–1.0 km diameter) plumes.

[35] The above results assume groundwater with a solute-free freezing point of 273 K. However, if the groundwater is a brine, *Travis and Feldman* [2009] found that the cryosphere could be reduced to a partially frozen zone ranging from a few tens to a few hundreds of meters thick. This also led to the formation of a number of narrow (~10 m diameter), vertical, ice-free "drainage pipes," spaced roughly 1 km apart, that rose to within several meters of the surface, providing a conduit for transporting concentrated brine back to the underlying subpermafrost aquifer.

[36] While it is unknown whether the conditions required for the hydrothermal convection of groundwater occur on Mars today, conditions were certainly more favorable and widespread in the past, when the mean values of lithospheric heat flow during the Noachian and Hesperian were estimated to have been as much as two to four times higher than today (Figure 2).

2.5. Description of the Crustal Model

[37] To investigate the extent, thermal structure, and evolution of the Martian cryosphere with time, we use a refinement of a one-dimensional finite difference thermal model developed by *Clifford and Bartels* [1986] to calculate diurnal and seasonal temperature variations (including the condensation of CO_2) over 5 year periods, at 10^3 year intervals, to determine the effects of long-term (~10^5–10^7 years) astronomically driven variations in insolation on subsurface temperature. Among the other factors taken into account by the model are: the temperature-dependent thermal properties of ice and rock; the desiccation state of the equatorial regolith; the composition of pore-filling ice (methane hydrate versus water ice); the effects of freezing point depressing salts; the decline of crustal porosity with depth; and two values of lithospheric heat flow (15 mW m^{-2} and 30 mW m^{-2}, the latter to permit more ready comparison with previously published estimates).

[38] For the purposes of these calculations, the model assumes that the temperature at the base of the cryosphere is defined everywhere by one of four isotherms. For a water-ice cryosphere we considered groundwater freezing temperatures corresponding to pure water (273 K) and eutectic solutions of NaCl (252 K) and $Mg(ClO_4)_2$ (203 K). For the case of a hydrate-rich cryosphere, we also considered a temperature of 303 K, a representative value for the base of the Hydrate Stability Zone (HSZ) for the pressure conditions expected at depths ≥ 10 km (see discussion in section 3.1). In reality, cryosphere basal temperatures below 273 K may be restricted to those locations where the base of the cryosphere is in direct contact with saline groundwater. Elsewhere, the hydrothermal circulation of vapor and condensed water through the vadose zone will likely deplete the intervening crust of freezing point depressing salts, resulting in a minimum cryosphere basal temperature near 273 K.

[39] The geologic characteristics of the model are as follows: Within the latitude range of ±40°, the diffusive instability of ground ice is expected to have led to the

desiccation of the equatorial regolith to an assumed maximum depth of 180 m at 0° latitude, 10 m at 40° latitude, ~1 m at 60° latitude, and 0.1 m at 70° latitude. Depths of this order are consistent with those predicted by most previous models of ground ice stability [*Clifford and Hillel*, 1983; *Fanale et al.*, 1986, *Zent et al.*, 1986; *Mellon and Jakosky*, 1995; *Mellon et al.*, 1997; *Schorghofer and Aharonson*, 2005] and, at high latitudes, with estimates of ground ice depth inferred from the analysis of the Gamma Ray Spectrometer and Neutron Spectrometer data [*Boynton et al.*, 2002; *Feldman et al.*, 2002; *Mitrofanov et al.*, 2002].

[40] The top 5 m of this crustal model are assumed to consist of a high-porosity granular material with an ice-free thermal conductivity of 0.06 W m^{-1} K^{-1}, consistent with a thermal inertia of 220 J m^{-2} K^{-1} $s^{-1/2}$ and with laboratory measurements of the thermal conductivity of similar materials under Mars atmospheric pressure [*Presley and Christensen*, 1997]. Beneath this initial surface layer, we assume the presence of a second layer, extending from a depth of 5–180 m, which encompasses that region of the deeper crust most susceptible to desiccation by the sublimation of equatorial ground ice. To investigate the sensitivity of our calculations to the assumed thermal properties of this region, we consider two lithologies: (1) "unconsolidated, porous volcanic or sedimentary rock" with a fixed, ice-free bulk thermal conductivity of 0.1 W m^{-1} K^{-1} (again, consistent with the lab measurements of *Presley and Christensen* [1997]) and (2) "consolidated volcanic rock" with a fixed, ice-free bulk thermal conductivity of 1 W m^{-1} K^{-1} (identical to the value for "dense rock" adopted by *Mellon et al.* [1997]). The porosity of both models is assumed to be the same (as intergrannular porosity in the unconsolidated material and as vesicles and fractures in the consolidated rock). For the sake of simplicity, the cryosphere models associated with these lithologies are hereafter referred to as our "low-k" and "high-k" models, where their given thermal conductivities apply solely to that portion of the regolith that is ice free (i.e., above the depth of the latitudinally variable sublimation front/ice table). Beneath the ice table, we assume that the crust is saturated with ice down to the base of the cryosphere, with a bulk thermal conductivity given everywhere by equation (2).

[41] Because we assume that the thermal conductivity of basalt and ice are the same, variations in saturated porosity beneath the ice table do not alter the effective thermal conductivity of our water-ice cryosphere. However, this is not the case if the volatile component of the cryosphere is gas hydrate, whose low thermal conductivity (0.5 W m^{-1} K^{-1}), is roughly constant over the range of temperatures characteristic of Mars [*Krivchikov et al.*, 2005]. Because this behavior differs from the temperature-dependent thermal conductivity of basalt, variations in saturated porosity can have a significant impact on the effective thermal conductivity of a gas hydrate cryosphere.

[42] To calculate the effect of such mixing, the variation of subsurface porosity with depth was modeled using the exponential decay relationship of *Clifford* [1993]

$$\Phi(z) = \Phi(0) \cdot \exp\left(\frac{-z}{D}\right), \quad (5)$$

where $\Phi(0)$ is the surface porosity (for which we assume values of 0.2 and 0.35), z is the depth in km, and D is the gravitationally scaled porosity decay constant which, for Mars, is estimated to be ~2.82 km [*Clifford*, 1993]. Using this relation, we then calculated the composite thermal conductivity of the basalt/gas hydrate cryosphere based on a geometric mixing rule, where $k_m\ (z,\ T) = k_h^{\Phi(z)} k_{(T)}^{(1-\Phi(z))}$. A mixing formula that gives values accurate to within 2% of those calculated using the slightly more accurate, but computationally demanding, quadratic expression of *Robertson and Peck* [1974].

[43] No attempt was made to simulate the dynamic redistribution of surface ice in response to climate change. Rather, fixed perennial polar caps, encompassing the area poleward of 80° latitude, were assumed. Diurnal, seasonal, and mean annual surface temperatures were then calculated at appropriate intervals based on the 20 Ma obliquity history of *Laskar et al.* [2004].

3. Results and Implications

[44] Here we present the results of our reexamination of the extent of the Martian cryosphere and its response to climate change. We then discuss the implications of these results for the continued survival of subpermafrost groundwater and its potential detection by the MARSIS radar sounder onboard the Mars Express spacecraft.

3.1. Depth of the Cryosphere and Its Response to Climate Change

[45] The depth of a water-ice cryosphere, for three groundwater freezing temperatures (273 K, 252 K, and 203 K), two values of mean global heat flow (15 mW m^{-2} and 30 mW m^{-2}) and two values of desiccated equatorial regolith thermal conductivity (0.1 W m^{-1} K^{-1} and 1.0 W m^{-1} K^{-1}) are presented in Figures 4a and 4b, over the latitude range of 0°–90°.

[46] As noted above, these depths were calculated based on surface temperatures derived from the 20 Ma nominal insolation history of *Laskar et al.* [2004], which represents a more relevant (and dynamic) boundary condition than the present-day mean annual surface temperatures previously assumed by *Clifford* [1993] and *Clifford and Parker* [2001]. Interestingly, although these astronomically driven changes in insolation have led to significant variations in mean annual surface temnperature over the last 20 Ma, the mean latitudinal surface temperature over this period is generally within a few degrees of the current annual mean (Figure 3).

[47] Figures 4a and 4b illustrate the potential range of depths for a water-ice cryosphere for various combinations of groundwater freezing point depression, heat flow, and assumed thermal properties. Figure 4a summarizes the results for our low-k (0.1 W m^{-1} K^{-1}) desiccated equatorial regolith model, while Figure 4b presents the results for our high-k (1. 0 W m^{-1} K^{-1}) model. A comparison of Figures 4a and 4b readily illustrates the considerable impact (Δz ~ 4 km) that a fine-grained, desiccated, low-conductivity regolith can have on reducing the maximum depth of the cryosphere near the equator, an impact that effectively vanishes by midlatitudes, as the depth of regolith desiccation declines.

[48] Although the order of magnitude range in thermal conductivity spanned by our low- and high-k regolith models covers a geologically realistic range, other investigators have

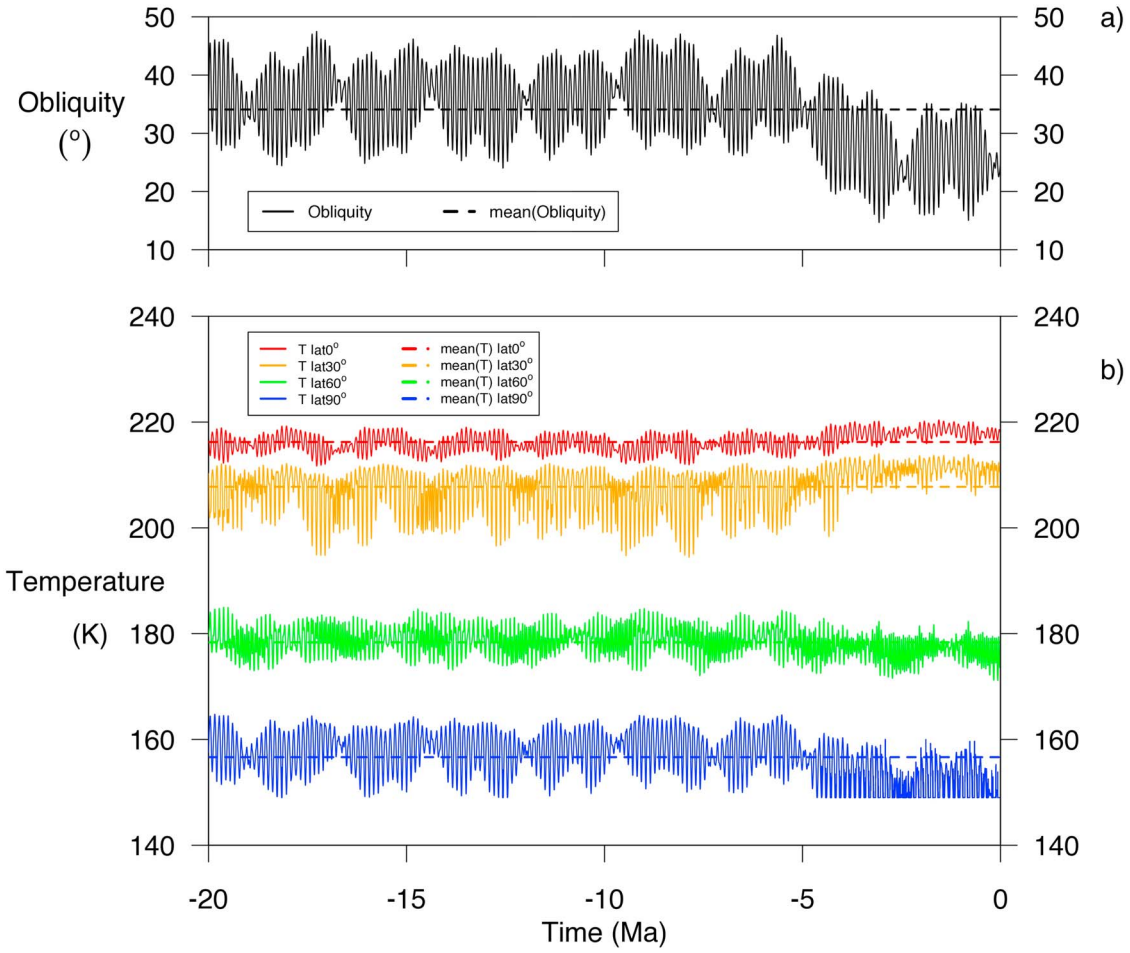


Figure 3. Obliquity-induced variations in mean surface temperature at four Mars latitudes over the past 20 Ma. (a) The 20 Ma nominal obliquity history of Mars [*Laskar et al.*, 2004]. (b) Corresponding variation in mean annual surface temperature at 0°, 30°, 60° and 90° latitude. Note that the corresponding 20 Ma mean surface temperatures (horizontal dashed lines) are 216 K for 0°, 208 K for 30°, 178 K for 60°, and 157 K for 90° for our model's assumed radiative and thermal properties, described in section 2.5.

considered fine-grained regoliths with even lower thermal conductivities. For example, *Mellon et al.* [1997] considered a "particulate" regolith with a thermal conductivity of only 0.02 W m^{-1} K^{-1}.

[49] *Wood and Griffiths* [2009] have gone a step further by considering how the periodic decrease in atmospheric pressure, associated with the growth of the seasonal polar caps at times of low obliquity, might result in a transient reduction in the thermal conductivity of the desiccated regolith above the ice table. They estimate that this effect is capable of reducing the thermal conductivity of a fine-grain (sand sized) regolith by a factor of 10 for as long as 3×10^4 years, which could impact the thermal structure of the crust to depths of ~1–10 km.

[50] Assuming a cryosphere with a basal temperature of 273 K, and the previous best estimate of lithospheric heat flow (Q_g = 30 mW m^{-2}), we find that the depth of the equatorial cryosphere ranges from ~0.5 km (for our low-k model, Figure 4a) to ~4.5 km (for our high-k model, Figure 4b). At 90° latitude, this depth increases to ~10.5 km, a result that because the polar cryosphere is expected to be fully satureated, is unaffected by the assumed lower thermal conductivity of the desiccated equatorial regolith. When Q_g is reduced to our present best estimate of 15 mW m^{-2}, it increases these estimated depths by approximately a factor of two.

[51] Similarly, if the base of the cryosphere is in contact with a eutectic brine of NaCl (i.e., with a freezing temperature of 252 K), it reduces equatorial cryosphere thicknesses to ~0.12 km (for the low-k model), to 2.6 km (for the high-k model) and yields a polar thickness of ~9.2 km (for both models), assuming a mean global heat flow of Q_g = 30 mW m^{-2}. As before, a heat flow of 15 mW m^{-2}, effectively doubles the expected depth of frozen ground.

[52] However, if sufficient perchlorate is present in the crust to lower the freezing point to 203 K, the cryosphere will be absent at all latitudes equatorward of ~35°, although it will still exist at higher latitudes, reaching a maximum thickness of between ~4.5 km (30 mW m^{-2}) to ~9 km (15 mW m^{-2}) at the poles.

[53] It is important to note, however, that in the real world the potential reduction of cryosphere thickness by the effects of salt (section 2.3) and the low-temperature hydrothermal convection of groundwater (section 2.4) will generally be

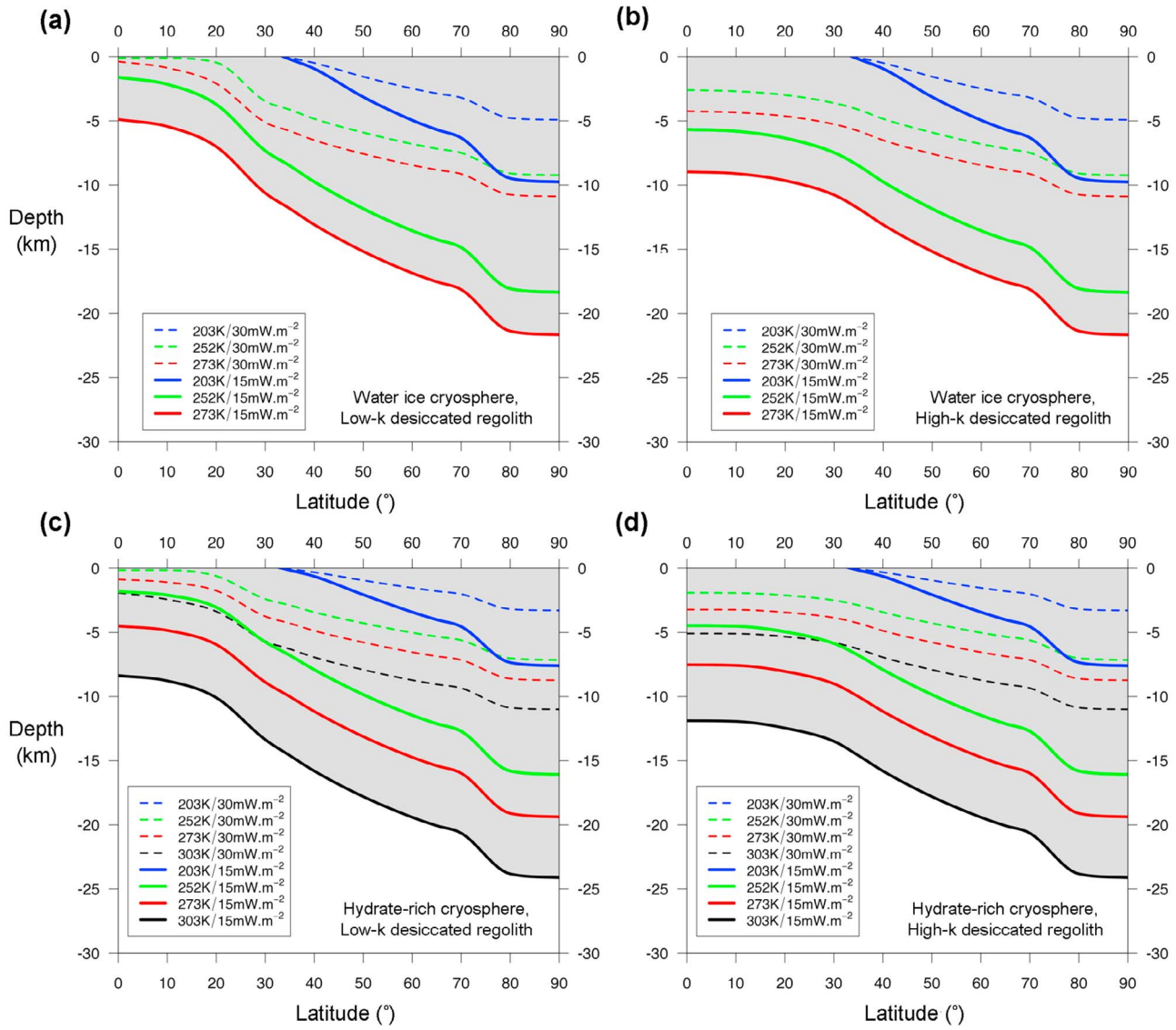


Figure 4. Latitudinal variation in the depth of a water-ice cryosphere for three different groundwater freezing temperatures (273, 252, and 203 K), two values of assumed lithospheric heat flow (15 mW m^{-2} and 30 mW m^{-2}), and two models of the thermal conductivity of the desiccated equatorial regolith for a (a) "low-k" model (0.1 W m^{-1} K^{-1}) and (b) a "high-k" model (1.0 W m^{-1} K^{-1}). (c and d) Subsurface extent of a gas hydrate cryosphere for the same variables in Figures 4a and 4b but assuming a basal temperature of 303 K, which approximates the base of the gas hydrate stability zone (HSZ) for the pressures conditions expected at depths of ≥ 10 km on Mars. See sections 2.5 and 3.1 for additional details.

restricted to those locations where the base of the cryosphere and groundwater are in direct contact (i.e., at low elevation). Where the base of the cryosphere rises above the water table (as is most probably does beneath high elevations, Figure 1), the geothermally induced circulation of H_2O vapor and condensate, over billions of years, is likely to have depleted the intervening crust of any high concentrations of freezing point depressing salts, maximizing the local thickness of frozen ground.

[54] Of course, the potential for the biotic or abiotic production of methane at depth raises the possibility that the chief volatile component of the cryosphere is gas hydrate, rather than water ice [*Fisk and Giovannoni*, 1999; *Max and Clifford*, 2000]. If so, the presence of gas hydrate (k_h = 0.5 W m^{-1} K^{-1}) has the potential to lower the effective thermal conductivity of the crust in proportion to its relative volumetric contribution.

[55] Figures 4c and 4d represent the gas hydrate equivalents of the water-ice cryospheres illustrated in Figures 4a and 4b, where we have assumed a surface porosity Φ (0) = 0.35, a crustal porosity profile given by equation (5), and that all of the available pore space between the ice table and base of the HSZ is completely saturated with hydrate. A surface porosity of 0.35 was chosen because it represents a realistic maximum value for the near surface of Mars when averaged over large (i.e., ~1 km^3) volumes. This maximizes the impact of gas hydrate on lowering the effective thermal

conductivity of the crust (versus the assumption of a surface porosity of 0.2 in Figures 4a and 4b).

[56] Note that while the lower effective thermal conductivity of a hydrate-saturated cryosphere means that the depth to any particular isotherm will be shallower than a cryosphere saturated with water ice, under high confining (lithostatice) pressure hydrate is stable to temperatures well in excess of 273 K [*Max and Clifford*, 2000]. The temperature that defines the base of the HSZ is dependent on the mean annual surface temperature, local geothermal gradient, confining pressure, and the salinity and composition of any other dissolved minerals present in the groundwater [*Max and Dillon*, 1998; *Max and Clifford*, 2000]. At the higher temperatures that characterize the region beneath the base of the HSZ, methane will exist either in solution with the local groundwater or as trapped pockets of pressurized gas.

[57] For a confining pressure of ~10^8 Pa, equivalent to the lithostatic pressure at a depth of ~10 km on Mars (assuming a crustal density of 2.5×10^3 kg m^{-3}), hydrate is stable to a maximum temperature of ~303 K [*Max and Clifford*, 2000, Figure 1], a value that for the purpose of illustration, we have adopted as constant in defining the maximum depth of the HSZ in Figures 4c and 4d. The resulting depths of the HSZ at the equator are ~1.9 km and ~5 km for our low- and high-k regolith models, respectively, assuming Q_g = 30 mW m^{-2}. These depths increase to ~8.3 km to ~12 km for a Q_g of 15 mW m^{-2}. The corresponding thickness of the HSZ at the poles is ~11.5 km (for Q_g = 30 mW m^{-2}) and ~23.5 km (for Q_g = 15 mW m^{-2}), the later is irrespective of which equatorial regolith model is used.

[58] Thus, despite the lower effective thermal conductivity of a hydrate-saturated cryosphere, the higher temperatures at which gas hydrate is stable mean that the depth to groundwater is actually greater for a hydrate cryosphere than that for a water-ice cryosphere with a basal temperature of 273 K (Figures 4a and 4b versus 4c and 4d). This assumes groundwater salinities that are roughly equivalent to terrestrial seawater, as the stability of hydrate in contact with eutectic solutions of perchlorate and other potential Martian salts is unknown. It also assumes that sufficient methane has been generated in the subsurface (by whatever process) to saturate the pore volume of the HSZ.

[59] Figure 5 illustrates the thermal response of a water-ice cryosphere (low-k model) to astronomically induced variations in insolation over the last 20 Ma [*Laskar et al.*, 2004], at four latitudes (0°, 30°, 60° and 90°). We find that at a latitude of 60°, climatic surface temperature variations over this time period have been minimal and have had no significant impact on the depth of the cryosphere. However, near the equator, the ~10° decline in mean obliquity over the past 6 Ma has increased the mean annual surface temperature by up to several degrees and reduced the maximum depth of the equatorial cryosphere by as much as ~500–600 m. At 90° latitude, this change in obliquity has reduced mean polar temperatures by ~5 K, increasing the depth of the polar cryosphere by as much as a km (a consequence of the higher thermal conductivity of the colder polar ice).

3.2. Implications for the Survival of Groundwater

[60] Although the outflow channels provide persuasive evidence that Mars possessed a sizable inventory of groundwater at the time of the Late Hesperian [*Carr*, 1986, 1996], the result of this and a previous study [*Clifford and Parker*, 2001] suggest the possibility that such a reservoir may no longer survive, a potential consequence of the progressive cold trapping of a once large inventory into the pore volume of the thickening cryosphere, as the planet's internal heat flow has declined with time.

[61] In the original calculations by *Clifford and Parker* [2001], it was found that depending on the assumed porosity profile of the crust, the freezing point of groundwater, and the rate of decline in mean crustal heat flow, an initial planetary inventory of 500 m of H_2O could have been fully cold trapped into the thickening cryosphere by the end of the Late Hesperian (~3 Ga), while, given an initial inventory of H_2O equivalent to a global ocean 1 km deep, the equivalent of up to several hundred meters of subpermafrost groundwater might still survive to the present-day.

[62] With the twofold increase in the potential maximum thickness of the cryosphere suggested here the prospects for the long-term survival of subpermafrost groundwater are in greater doubt. Table 1 presents estimates of the potential storage capacity of the Martian cryosphere (expressed as the thickness of an equivalent global layer of water) for the three values of assumed groundwater freezing temperature, two values of crustal heat flow, two crustal porosity profiles, and both the low- and high-k equatorial regolith models considered in this study. As a point of comparison, note that for Φ (0) = 0.20 and 0.35, the total pore volume of the crust is equivalent to a global ocean ~615 m and ~1060 m deep, respectively, results that reflect the integrated pore volume to a depth of 26.5 km (the gravitationally scaled equivalent of the 10 km depth of the Earth's crust for which there is evidence of hydraulic continuity [*Manning and Ingebritsen*, 1999]).

[63] These results indicate that even with the assumption of a high (~30 mW m^{-2}) heat flow and a groundwater composition equivalent to a eutectic solution of NaCl, it is highly unlikely that any portion of an initial planetary inventory of H_2O equal to *Carr*'s [1986] lower estimate of a ~500 m GEL would survive to present-day as groundwater, a probability that becomes a virtual certainty if the current mean global heat flow is as low as the 15 mW m^{-2} value suggested here.

[64] However, it might be argued that if Martian groundwater were rich in perchlorate (with a eutectic of 203 K), some might survive to the present-day, even if the initial planetary inventory of H_2O was small. This conclusion appears to follow from the small pore volumes associated with a 203 K cryosphere, which range from a ~135–360 m GEL (Table 1). But this estimate of cryosphere pore volume assumes that the base of the cryosphere is everywhere in contact with a eutectic solution of perchlorate. In the absence of a more accurate understanding of the actual spatial distribution of groundwater, this assumption provides a simple and consistent way to assess the potential impact of groundwater freezing point depression on cryosphere pore volume. However, as seen in Figure 1, the actual relationship between the distribution of groundwater and the base of the cryosphere is likely to be quite different.

[65] Indeed, if Martian groundwater is both abundant and saturated with perchlorate, thermal and hydraulic conditions

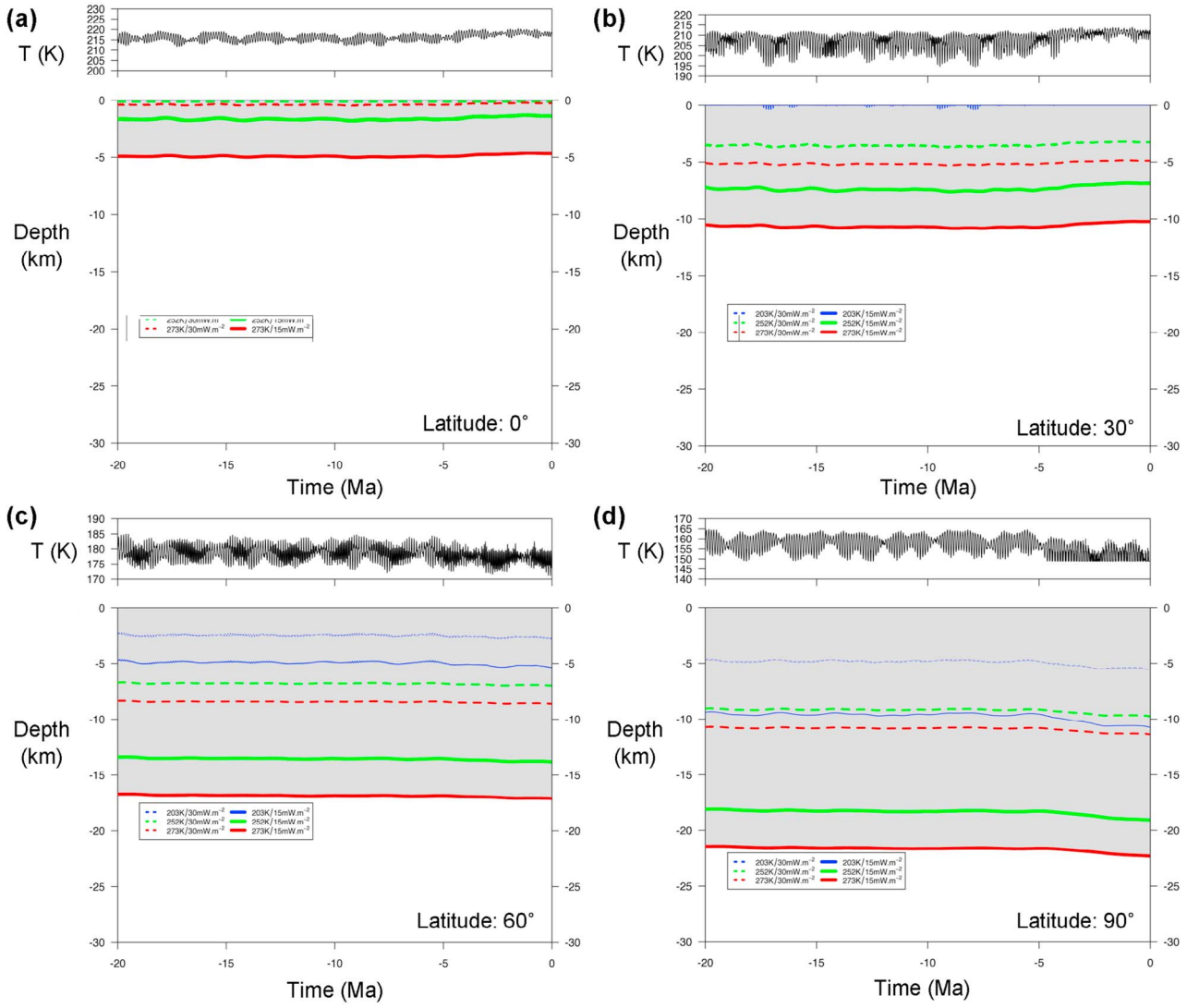


Figure 5. For latitudes (a) 0°, (b) 30°, (c) 60°, and (d) 90°, (top) the astronomically induced variations in mean annual surface temperature versus time and (bottom) the corresponding variation in the depth to the base of a water ice cryosphere are illustrated. The results are presented for three different groundwater freezing temperatures (273, 252, and 203 K) and two values of assumed lithospheric heat flow (15 and 30 mW m^{-2}) for the low-k (0.1 W m^{-1} K^{-1}) equatorial regolith model described in section 2.5. Surface and subsurface temperatures are calculated based on the 20 Ma nominal obliquity history of *Laskar et al.* [2004]. Note that the amplitude of the variation in the depth of a particular isotherm, declines for the warmer isotherms at depth, for those associated with the same heat flow. Climatic variations in the depth of a particular isotherm are necessarily greater for models that assume a smaller heat flow versus a larger one. The most notable trend evident in these climate histories is a slight surface warming at equatorial latitudes (Figures 5a and 5b) and slight cooling at the poles (Figure 5d), over the last 6 Ma. The change in the depth of the 273 K isotherm that corresponds to this change in surface temperature amounts to just a few hundred meters at the equator and ~500–600 m at 30° and 90° latitude, assuming a heat flow of 15 mW m^{-2}. The variations in the depth of the 273 K isotherm are roughly half as great for a heat flow of 30 mW m^{-2}.

necessarily constrain the location of the planetary water table to lie at, or below, the planet's minimum surface elevation. This is because the mean annual surface temperature at all latitudes equatorward of 35° exceeds the 203 K eutectic temperature of a perchlorate brine, effectively eliminating the hydraulic confining ability of the cryosphere, wherever it is in contact with groundwater, at these latitudes. Without invoking implausibly low values of near-surface crustal permeability, the absence of the cryosphere as a hydraulic barrier, in combination with the presence of a high water table (i.e., relative to the planet's minimum surface elevation), would allow groundwater to discharge

Table 1. Total Pore Volume of Cryosphere: Depth of Global Equivalent Layer of Water[a]

Basal Melting/Groundwater FreezingTemperature (K)	Q_g = 15 mW m^{-2} (High k Equatorial Regolith)		Q_g = 30 mW m^{-2} (Low k Equatorial Regolith)	
	Φ (0) = 0.20	Φ (0) = 0.35	Φ (0) = 0.20	Φ (0) = 0.35
273	585	1025	435	760
252	565	990	340	595
203	205	360	135	235

[a]Pore volumes reflect the integrated porosity of the crust, expressed in terms of a global equivalent layer (GEL) of water (in m), between the surface and the depth of the indicated isotherm, based on a porosity profile given by equation (5). Pore volumes are listed for two combinations of lithospheric heat flow and low- (0.1 W m^{-1} K^{-1}) and high-k (1.0 W m^{-1} K^{-1}) models of the desiccated equatorial regolith which have been chosen to represent the likely minimum and maximum extents of the cryosphere at these latitudes. On Earth, there is evidence of hydraulic continuity extending down to a depth of ~10 km [*Manning and Ingebritsen*, 1999]. Gravitational scaling this result to Mars suggests that the crust will remain permeable to a depth of ~26.5 km. For reference purposes, the total pore volume of the Martian crust, integrated down to this depth, is 615 m for Φ (0) = 0.20 and 1060 m for Φ (0) = 0.35. The actual values of crustal porosity are likely to exhibit significant spatial variability [*Clifford*, 1993; *Clifford and Parker*, 2001].

onto the surface, resulting in springs, playas, and standing bodies of water, throughout the planet's lowest elevations, evidence that is not observed.

[66] Given that (1) most of the available pore volume of the Martian crust is expected to lie within a few kilometers of the surface (i.e., equation (5)), (2) the hypsometric characteristics of Martian topography suggest that the bulk of this crustal pore volume lies at an absolute elevation well above the global minimum [*Smith et al.*, 2003], and (3) the necessity that the height of the planetary water table for perchlorate-saturated groundwater must lie at or below the planet's minimum surface elevation (to avoid discharge from a lack of confinement), it follows that only ~20% of the total pore volume of a 273 K cryosphere would be impacted by the presence of perchlorate-saturated groundwater. This leaves ~80% of that pore volume available as cold trap for the planet's inventory of H_2O. Thus, if the planetary inventory of water is small (i.e., $\leq$500 m), little if any is expected to survive as subpermafrost groundwater, other than that which may be transiently produced by volcanism, magmatism, and large impacts.

[67] The results in Table 1 suggests that the prospects for the survival of groundwater are more promising if the planetary inventory of H_2O is closer to *Carr*'s [1986, 1996] upper estimate of an ~1 km GEL. In addition, moderately elevated groundwater tables, relative to the global topography, are possible as long as the freezing point of the groundwater is high enough to permit a sufficient thickness of frozen ground to ensure hydraulic confinement [*Clifford and Parker*, 2001].

[68] From these results, the present state of groundwater on Mars appears bracketed by two extremes: one in which a small initial inventory of H_2O, combined with the progressive cooling of the crust, eventually cold trapped all of the planet's groundwater into the cryosphere and, another, where the original inventory of H_2O on Mars was sufficiently large that a sizable reservoir (up to several hundred meters) of subpermafrost groundwater may still survive to the present-day.

[69] In the latter case, recent estimates of the planet's present global heat flow indicate that if groundwater still persists, it will generally reside at depths $\geq$ 5 km beneath the local surface (Figure 4), or roughly twice as deep as previously thought [*Clifford*, 1993; *Clifford and Parker*, 2001]. But as discussed below, natural variations in crustal thermal conductivity, heat flow, and groundwater composition, may permit isolated occurrences of groundwater to exist at significantly shallower depths.

3.3. Implications for the Detection of Subpermafrost Groundwater by Radar Sounding

[70] The greater the thickness of the Martian cryosphere, the greater the technical challenge of detecting any groundwater that might lie beneath it. The MARSIS orbital radar sounder, onboard ESA's Mars Express spacecraft, was designed to investigate the Martian ionosphere and the geological and hydrological structure of the subsurface, with a particular emphasis on the potential detection of deep subpermafrost groundwater [*Picardi et al.*, 2003, 2004]. MARSIS is a multifrequency, coherent pulse, synthetic aperture radar sounder that operates by detecting reflections which are generated at the interface between two materials of differing dielectric properties.

[71] Geologic materials (including water and ice) have the following two properties that influence their interaction with the electromagnetic waves: (1) their electrical permittivity (which, when measured relative to the value for air, is called the dielectric constant) and (2) their magnetic permeability. Both parameters are complex values, with the real part a measure of how much energy is stored and reradiated by the material, while the imaginary part reflects the amount of energy that is lost in the material due to thermal effects associated with wave propagation and diffusion [*Campbell*, 2002]. The dielectric constant of geologic materials is a complicated function of their composition, grain size, porosity, temperature, and radar frequency. However, with the exception of materials possessing high concentrations of hematite and magnetite, most geologic materials have no measurable magnetic properties.

[72] The interactions of radar waves with planetary surfaces, and their propagation into the subsurface, are largely determined by the dielectric properties of the materials they encounter. When a radar pulse reaches the boundary between two materials with differing dielectric properties (such as the atmosphere and ground), a portion of the incident energy is reflected backward, while the remainder continues to propagate into the subsurface, where it may suffer additional losses due to scatter by imbedded objects and absorption by the host material itself. As successive dielectric interfaces are encountered, the signal experiences

further losses that affect both the transmitted and reflected portions of the signal. This continues until the reflected signal can no longer be detected above the background noise. The ability of a GPR to investigate the geologic and hydrologic properties of the subsurface is therefore critically dependent on the relative dielectric contrast between any two materials, among the greatest being that between liquid water and dry or frozen rock.

[73] MARSIS operates at frequencies of ~2–5 MHz, giving it a theoretical ability to detect the presence of subpermafrost groundwater, under ideal sounding conditions, at depths of up to ~3–5 km beneath the Martian surface [*Picardi et al.*, 2004]. Such conditions include a sharp transitional boundary (over a vertical distance less than half the radar wavelength in the ground, or (for the case of MARSIS) roughly ~25–50 m), a saturated crustal porosity > 10%, and an r.m.s. surface roughness of < 05° (which characterize ~20% of the planet [*Picardi et al.*, 2003]).

[74] In practice, MARSIS has achieved this level of sounding performance only in select environments, which include the ice-rich (and, thus, low dielectric loss) north and south PLD, as well as several other sites at lower latitudes. Of the latter, the most notable is the Medusae Fossae Formation, whose radar propagation characteristics are consistent with a composition ranging from a dry, high-porosity pyroclastic deposit at one extreme to an ice-rich sedimentary deposit at the other, potentially formed by the redistribution of polar volatiles at times of high obliquity [*Watters et al.*, 2007b]. Hints of several other moderately deep reflectors have also been found in the vicinity of Ma'adim Vallis, where there is evidence that they may originate from lithologic interfaces [*White et al.*, 2009].

[75] The absence of more widespread evidence of deep reflectors, potentially indicative of the presence of subpermafrost groundwater, has at least four possible explanations: (1) Subpermafrost groundwater may no longer survive on Mars, a once large inventory having been cold trapped into the growing pore volume of the thickening cryosphere or lost by other processes (e.g., chemical weathering or exospheric escape). (2) Groundwater is present but the cryosphere is deeper than previously expected, placing groundwater beyond the maximum sounding depth of MARSIS. (3) The presence of thin films of liquid water in the lower cryosphere, or within the vadose zone above a subpermafrost groundwater table, has reduced the dielectric contrast necessary to produce a detectable reflection [*Beaty et al.*, 2001; *LeGall et al.*, 2007]. (4) The dielectric loss and scattering properties of the subsurface are more attenuating than previously believed, resulting in a shallower than expected MARSIS sounding performance [*Heggy et al.*, 2006; *Grimm et al.*, 2006; *Boisson et al.*, 2009].

[76] Which one (or combination) of these explanations is responsible for the null results from MARSIS, and whether their influence is global or varies from location to location, is unknown. But the likely nature and extent of the Martian cryosphere are critical considerations in the analysis and interpretation of the MARSIS data. A factor of two increase in the potential depth of the cryosphere is an especially critical concern, raising questions about whether groundwater still persists at depth and if it does, whether it lies within the detectable reach of MARSIS. Given such concerns, what geologic characteristics must be considered in identifying those locations that optimize the chance for a successful detection?

[77] The results of an orbital radar sounding investigation constrain the occurrence of groundwater when (1) there is reason to believe that the groundwater should occur within the detectable range of the instrument and (2) there is evidence that the instrument has reliably achieved this depth of sounding over a representative fraction of the area where groundwater is most likely to occur. Unless both of these conditions are satisfied, a search that yields a null result, by itself, places no constraints on the presence of groundwater.

[78] Comparing the estimates of mean cryosphere thickness presented in Figure 4 with the estimated ~3–5 km maximum sounding depth of MARSIS, suggests that the detection of subpermafrost groundwater on Mars, even at the equator, will be a challenging task. However, as discussed in section 2, natural variations in the range of crustal thermal properties are likely to result in significant (at least ± 50%) local variations in cryosphere thickness about the zonal mean.

[79] As evident from consideration of the relationship between the base of the cryosphere and groundwater, illustrated in Figure 1, the locations that provide the best opportunity for detecting groundwater are those that combine low latitude (minimizing the thickness of frozen ground, due to higher mean annual surface temperatures) and low elevation (minimizing the depth to a water table in hydrostatic equilibrium). This reasoning is strengthened by the fact that it is at low elevation that the cryosphere is most likely in direct contact with any underlying reservoir of subpermafrost groundwater, where its thickness may be reduced by the effects of freezing point depressing salts, the low-temperature hydrothermal convection of groundwater, or a combination of both, which may result in spatial variations in heat flow that dramatically reduce the local depth of frozen ground [*Travis et al.*, 2003; *Travis and Feldman*, 2009]. The specific locations that best satisfy the criteria of low latitude and low elevation are: the eastern interior of Valles Marineris, southern Amazonis Planitia, Isidis Planitia, the northwest interior of Hellas, and Athabasca Valles, a region to the southeast of Elysium [*Clifford and Parker*, 2001, Table 6].

[80] *Boisson et al.* [2009] have reported on the results of their analysis of a MARSIS radar data acquired over one of these sites, Athabasca Valles (5°N, 150°E). In addition to being a low-latitude, low-elevation site, this region is also extremely smooth at the wavelengths employed by MARSIS (~100 m), minimizing the potential for off-nadir reflections from the local topography (also known as "clutter") that might degrade the signal-to-noise ratio and complicate the identification of groundwater. Despite this combination of characteristics, the Athabasca radargram is essentially featureless, containing no evidence of a deep reflector [*Boisson et al.*, 2009].

[81] Although this result appears most consistent with either the absence of groundwater or a cryosphere thickness that exceeds the theoretical ~3–5 km maximum sounding depth of MARSIS, further analysis suggests a different explanation. *Boisson et al.* [2009] found that the decay characteristics of the backscattered radar signal indicate that the local radar propagation characteristics of the subsurface are highly attenuating (equivalent to those of terrestrial

volcanic materials [*Heggy et al.*, 2006]), resulting in maximum penetration depth of ≤ 220 m. Because it is not yet known how representative of the Martian subsurface these characteristics may be, more comprehensive investigations of Athabasca and four other low-elevation, near-equatorial sites are currently underway.

[82] While orbital radar sounding investigations, like MARSIS, can conduct a global survey of Mars, at moderate spatial resolution, on a timescale of several years, their sensitivity is necessarily limited by their altitude, relative motion with respect to the planet's surface, and the necessity of having to sound through the Martian ionosphere. In contrast, a radar sounder, operating from a fixed lander, at the same frequency as MARSIS, can achieve a 90 dB improvement in sensitivity by its ability to perform many coherent additions of the reflected signal, which can dramatically improve signal to noise [*Ciarletti et al.*, 2003; *LeGall et al.*, 2006, 2008]. The trade-off for this improvement in sensitivity is that areal coverage provided by a sounder on a fixed lander is limited to a single point on the planet's surface (or up to several points, if the sounder is included as part of the payload of a multistation geophysical network [*Berthelier et al.*, 2003]). For this reason, landed investigations are best employed following an initial orbital reconnaissance, such as the one now being conducted by MARSIS, which can help identify those sites whose subsurface propogation characteristics are best suited to deep sounding. Ultimately, it will likely require a synthesis of data from radar sounders and other geophysical techniques [e.g., *Tittmann*, 1979; *Romig et al.*, 1983; *Goldman and Neubauer*, 1994; *Grimm*, 2002, 2003], obtained at multiple well-targeted sites across the planet to assess the presence and fate of groundwater on Mars.

4. Conclusions

[83] Various lines of evidence suggest that at the time of the Late Hesperian, Mars possessed a planetary inventory of water equal to a global ocean ~0.5–1 km deep, much of which is believed to have been stored as ground ice and groundwater in the subsurface. The potential survival of groundwater to the present-day has important implications for understanding the geological, hydrological and mineralogical evolution of the planet, as well as the potential survival of native Martian life. The two most important factors affecting the persistence of groundwater on Mars are the depth and pore volume of the cryosphere.

[84] To date, the orbital radar sounding data from MARSIS has provided little evidence of any deep reflectors potentially indicative of subpermafrost groundwater. Here we have examined two (of several) possible explanations for this lack of evidence: (1) that subpermafrost groundwater no longer survives on Mars or (2) that groundwater is present, but that a thicker than expected cryosphere has restricted its occurrence to depths that exceed the estimated ~3–5 km maximum sounding depth of MARSIS.

[85] Recent estimates of Martian geothermal heat flow, derived from rheologic estimates of the thickness of the elastic lithosphere, suggest a present-day value only half as great as previously thought, effectively doubling the expected thickness of the cryosphere and depth to groundwater. Our analysis suggests that the zonally averaged thickness of the cryosphere may vary from 0–9 km at the equator to ~10–22 km at the poles, depending principally on the availability of potent freezing point depressing salts, such as perchlorate. If Martian groundwater is perchlorate rich, then the absence of active springs, playas, and ponded surface water, constrains the depth of any planetary water table to lie below the planet's lowest elevations.

[86] Combining reasonable estimates of crustal porosity with our calculated range of cryosphere depths suggests that for a present-day heat flow of ~15 mW m^{-2}, the total pore volume of the Martian cryosphere is sufficient to cold trap ~0.5 km GEL of H_2O, equivalent to *Carr*'s [1986, 1996] lower estimate of the planetary inventory of water. However, if the planetary inventory is as great as Carr's maximum estimate of a ~1 km GEL, then we find that up to several hundreds of meters of groundwater may still survive at depth.

[87] Although the presence of a deep cryosphere diminishes the likelihood of a successful detection of groundwater by orbital radar sounding, local differences in lithospheric heat flow and crustal thermal properties (including the potential effects of potent freezing point depressing salts and the low-temperature hydrothermal convection of groundwater), may result in significant spatial variations in cryosphere thickness, especially where the cryosphere and groundwater are in contact, a condition that appears most likely at low latitude and low elevation. A preliminary analysis of MARSIS radar sounding data over one such site, Athabasca Valles, has revealed no evidence of a deep reflector potentially indicative of subpermafrost groundwater. While this result is consistent with several potential explanations, analysis of the characteristics of the backscatted echo indicate that it most probably results from the presence of highly attenuating subsurface conditions that limit the local maximum depth of radar sounding to ≤ 220 m.

[88] Which one (or combination) of explanations discussed here is responsible for the lack of deep reflectors on Mars is unknown. But our revised estimates of cryosphere depth suggest that a successful detection of subpermafrost groundwater, outside of those areas on Mars that combine low latitude and low elevation, is unlikely. In an effort to better constrain this problem, a more comprehensive investigation of the MARSIS sounding data obtained over Athabasca Valles, and four other low-elevation, near-equatorial sites, is currently underway.

[89] **Acknowledgments.** We are grateful to Keith Harrison and another anonymous reviewer whose comments and suggestions greatly assisted the revision of the manuscript. The work by S. Clifford was supported by the Lunar and Planetary Institute and a grant from NASA's MARSIS Participating Scientist Program. Additional French support was provided by CNES and by a MRT Ph.D. grant for J. Boisson. This is LPI contribution 1495.

References

Beaty, D. W., S. M. Clifford, P. Gogineni, R. Grimm, C. Leuschen, G. R. Olhoeft, K. Raney, and A. Safaeinili (2001), Report of the virtual instrument science definition team on: Facility Orbital Radar Sounder Experiment for MRO 2005 (FORSE), report, NASA, Washingon, D. C. (Available at http://www.lpi.usra.edu/meetings/geomars2001/virtual.pdf.)

Berthelier, J. J., et al. (2003), GPR, a ground-penetrating radar for the Netlander mission, *J. Geophys. Res.*, *108*(E4), 8027, doi:10.1029/2002JE001866.

Blackwell, D. D. (1971), The thermal structure of the continental crust, in *The Structure and Physical Properties of the Earth's Crust*, *Geophys. Monogr. Ser.*, vol. 14, edited by J. G. Heacock, pp. 169–184, AGU, Washington, D. C.

Boisson, J., et al. (2009), Sounding the subsurface of Athabasca Valles using MARSIS radar data: Exploring the volcanic and fluvial hypotheses for the origin of the rafted plate terrain, *J. Geophys. Res.*, *114*, E08003, doi:10.1029/2008JE003299.

Boynton, W. V., et al. (2002), Distribution of hydrogen in the near surface of Mars: Evidence for subsurface ice deposits, *Science*, *297*, 81–85, doi:10.1126/science.1073722.

Brace, W. F. (1980), Permeability of crystalline and argillaceous rocks, *Int. J. Mech. Min. Sci. Geomech. Abstr.*, *17*, 241–251, doi:10.1016/0148-9062(80)90807-4.

Brace, W. F. (1984), Permeability of crystalline rocks: New *in situ* measurements, *J. Geophys. Res.*, *89*, 4327–4330, doi:10.1029/JB089iB06p04327.

Brass, G. W. (1980), Stability of brines on Mars, *Icarus*, *42*, 20–28, doi:10.1016/0019-1035(80)90237-7.

Burt, D. M., and L. P. Knauth (2003), Electrically conducting, Ca-rich brines, rather than water, expected in the Martian subsurface, *J. Geophys. Res.*, *108*(E4), 8026, doi:10.1029/2002JE001862.

Campbell, B. A. (2002), *Radar Remote Sensing of Planetary Surfaces*, Cambridge Univ. Press, Cambridge, U. K.

Carr, M. H. (1979), Formation of Martian flood features by release of water from confined aquifers, *J. Geophys. Res.*, *84*, 2995–3007, doi:10.1029/JB084iB06p02995.

Carr, M. H. (1986), Mars: A water-rich planet?, *Icarus*, *68*, 187–216, doi:10.1016/0019-1035(86)90019-9.

Carr, M. H. (1996), *Water on Mars*, 229 pp., Oxford Univ. Press, New York.

Carr, M. H. (1999), Retention of an atmosphere on early Mars, *J. Geophys. Res.*, *104*, 21,897–21,909, doi:10.1029/1999JE001048.

Catling, D. C., M. W. Claire, R. C. Quinn, K. J. Zahnle, B. C. Clark, S. Kounaves, and M. H. Hecht (2009), Possible atmospheric origins of perchlorate on Mars, *Lunar Planet. Sci.*, *XXXX*, abstract 1567.

Ciarletti, V., B. Martinat, A. Reineix, J. J. Berthelier, and R. Ney (2003), Numerical simulation of the operation of the GPR radar on Netlander, *J. Geophys. Res.*, *108*(E4), 8028, doi:10.1029/2002JE001867.

Clark, B. C. (1978), Implications of abundant hygroscopic minerals in the Martian regolith, *Icarus*, *34*, 645–665, doi:10.1016/0019-1035(78)90052-0.

Clark, B. C., and D. C. Van Hart (1981), The salts of Mars, *Icarus*, *45*, 370–378, doi:10.1016/0019-1035(81)90041-5.

Clark, B. C., et al. (2005), Chemistry and mineralogy of outcrops at Meridiani Planum, *Earth Planet. Sci. Lett.*, *240*, 73–94, doi:10.1016/j.epsl.2005.09.040.

Clauser, C., and E. Huenges (1995), The thermal conductivity of rocks and minerals, in *Rock Physics and Phase Relations: A Handbook of Physical Constants*, *AGU Ref. Shelf Ser.*, vol. 3, edited by T. J. Ahrens, pp. 105–126, AGU, Washington, D. C.

Clifford, S. M. (1991), The role of thermal vapor diffusion in the subsurface hydrologic evolution of Mars, *Geophys. Res. Lett.*, *18*, 2055–2058, doi:10.1029/91GL02469.

Clifford, S. M. (1993), A model for the hydrologic and climatic behavior of water on Mars, *J. Geophys. Res.*, *98*, 10,973–11,016, doi:10.1029/93JE00225.

Clifford, S. M. (1998), Mars: The effect of stratigraphic variations in regolith diffusive properties on the evolution and vertical distribution of equatorial ground ice, *Lunar Planet. Sci.*, *XXVIII*, abstract 1922.

Clifford, S. M., and C. J. Bartels (1986), The Mars Thermal Model "Marstherm," a FORTRAN 77-finite differences program designed for general distribution, *Lunar Planet. Sci.*, *XVII*, 142–143.

Clifford, S. M., and D. Hillel (1983), The stability of ground ice in the equatorial region of Mars, *J. Geophys. Res.*, *88*, 2456–2474, doi:10.1029/JB088iB03p02456.

Clifford, S. M., and T. J. Parker (2001), The evolution of the Martian hydrosphere: Implications for the fate of a primordial ocean and the current state of the Northern Plains, *Icarus*, *154*, 40–79, doi:10.1006/icar.2001.6671.

Craddock, R. A., and R. Greeley (2009), Minimum estimates of the amount and timing of gases released into the Martian atmosphere from volcanic eruptions, *Icarus*, *204*, 512–526, doi:10.1016/j.icarus.2009.07.026.

Craddock, R. A., and A. D. Howard (2002), The case for rainfall on a warm, wet early Mars, *J. Geophys. Res.*, *107*(E11), 5111, doi:10.1029/2001JE001505.

Craddock, R. A., and T. Maxwell (1993), Geomorphic evolution of the Martian highlands through ancient fluvial processes, *J. Geophys. Res.*, *98*, 3453–3468, doi:10.1029/92JE02508.

Davidson, D. (1983), Gas hydrates as clathrate ices, in *Natural Gas Hydrates-Properties, Occurrence and Recovery*, edited by J. L. Cox, pp. 1–16, Butterworth, Woburn, Mass.

Ericksen, G. E. (1981), Geology and origin of the Chilean nitrate deposits, *U.S. Geol. Surv. Prof. Pap.*, *1188*, 366–374.

Fairén, A. G., A. F. Davila, L. Gago-Duport, R. Amils, and C. P. McKay (2009), Stability against freezing of aqueous solutions on early Mars, *Nature*, *459*, 401–404, doi:10.1038/nature07978.

Fanale, F. P. (1976), Martian volatiles: Their degassing history and geochemical fate, *Icarus*, *28*, 179–202, doi:10.1016/0019-1035(76)90032-4.

Fanale, F. P., J. R. Salvail, A. P. Zent, and S. E. Postawko (1986), Global distribution and migration of subsurface ice on Mars, *Icarus*, *67*, 1–18, doi:10.1016/0019-1035(86)90170-3.

Feldman, W. C., et al. (2002), Global distribution of neutrons from Mars: Results from Mars Odyssey, *Science*, *297*(5578), 75–78, doi:10.1126/science.1073541.

Fisk, M. R., and S. J. Giovannoni (1999), Sources of nutrients and energy for a deep biosphere on Mars, *J. Geophys. Res.*, *104*, 11,805–11,815, doi:10.1029/1999JE900010.

Formisano, V., S. Atreya, T. Encrenaz, N. Ignatiev, and M. Giuranna (2004), Detection of methane in the atmosphere of Mars, *Science*, *306*, 1758–1761, doi:10.1126/science.1101732.

Goldman, M., and F. M. Neubauer (1994), Groundwater exploration using integrated geophysical techniques, *Surv. Geophys.*, *15*, 331–361, doi:10.1007/BF00665814.

Grimm, R. E. (2002), Low-frequency electromagnetic exploration for groundwater on Mars, *J. Geophys. Res.*, *107*(E2), 5006, doi:10.1029/2001JE001504.

Grimm, R. E. (2003), A comparison of time domain electromagnetic and surface nuclear magnetic resonance sounding for subsurface water on Mars, *J. Geophys. Res.*, *108*(E4), 8037, doi:10.1029/2002JE001882.

Grimm, R. E., E. Heggy, S. Clifford, C. Dinwiddie, R. Mcginnis, and D. Farrell (2006), Absorption and Scattering in Ground Penetrating Radar: Analysis of the Bishop Tuff, *J. Geophys. Res.*, *111*, E06S02, doi:10.1029/2005JE002619.

Gulick, V. C. (1998), Magmatic intrusions and a hydrothermal origin for fluvial valley on Mars, *J. Geophys. Res.*, *103*, 19,365–19,387, doi:10.1029/98JE01321.

Hartmann, W., and G. Neukum (2001), Cratering chronology and the evolution of Mars, *Space Sci. Rev.*, *96*, 165–194, doi:10.1023/A:1011945222010.

Hecht, M. H., et al. (2009), Detection of perchlorate and the soluble chemistry of Martian soil at the Phoenix lander site, *Science*, *325*, 64–67, doi:10.1126/science.1172466.

Heggy, E., S. M. Clifford, R. E. Grimm, C. L. Dinwiddie, D. Y. Wyrick, and B. E. Hill (2006), Ground-penetrating radar sounding in mafic lava flows: Assessing attenuation and scattering losses in Mars-analog volcanic terrains, *J. Geophys. Res.*, *111*, E06S04, doi:10.1029/2005JE002589.

Hobbs, P. V. (1974), *Ice Physics*, Clarendon, Oxford, U. K.

Hunten, D. M. (1979), Possible oxidant sources in the atmosphere and surface of Mars, *J. Mol. Evol.*, *14*, 71–78, doi:10.1007/BF01732369.

Kargel, J. S., and J. I. Lunine (1998), Clatherate hydrates on Earth and in the solar system, in *Solar System Ices*, edited by B. Schmidt et al., pp. 97–117, Kluwer Acad., Dordrecht, Netherlands.

Krasnopolsky, V. A., J. P. Maillard, and T. C. Owen (2004), Detection of methane in the Martian atmosphere: Evidence for life?, *Icarus*, *172*, 537–547, doi:10.1016/j.icarus.2004.07.004.

Krivchikov, A. I., B. Y. Gorodilov, O. A. Korolyuk, V. G. Manzhelii, H. Conrad, and W. Press (2005), The themal conductivity of methane hydrate, *J. Low Temp. Phys.*, *139*, 693–702, doi:10.1007/s10909-005-5481-z.

Kuzmin, R. O. (1983), *Cryolithosphere of Mars*, Nauka, Moscow.

Laskar, J., and P. Robutel (1993), The chaotic obliquity of the planets, *Nature*, *361*, 608–612, doi:10.1038/361608a0.

Laskar, J., A. C. M. Correia, M. Gastineau, F. Joutel, B. Levrard, and P. Robutel (2004), Long term evolution and chaotic diffusion of the insolation quantities of Mars, *Icarus*, *170*, 343–364, doi:10.1016/j.icarus.2004.04.005.

Lee, Y., and D. Deming (1998), Evaluation of thermal conductivity temperature corrections applied in terrestrial heat flow studies, *J. Geophys. Res.*, *103*, 2447–2454, doi:10.1029/97JB03104.

Le Gall, A., A. Reineix, V. Ciarletti, J. J. Berthelier, R. Ney, F. Dolon, and C. Corbel (2006), An estimation of the electrical characteristics of planetary shallow subsurfaces with TAPIR antennas, *J. Geophys. Res.*, *111*, E06S06, doi:10.1029/2005JE002595.

Le Gall, A., S. M. Clifford, E. Heggy, V. Ciarletti, and D. Mukherjee (2007), Electromagnetic investigations of a deep water table in the west Egyptian desert: Lithologic and geothermal vapor effects on crustal resistivity and GPR performance, *Lunar Planet. Sci.*, *XXXVIII*, abstract 1338.

Le Gall, A., V. Ciarletti, J.-J. Berthelier, A. Reineix, C. Guiffaut, R. Ney, F. Dolon, and S. Bonaimé (2008), An imaging HF GPR using stationary antennas: Experimental validation over the Antarctic Ice Sheet, *IEEE Trans. Geosci. Remote Sens.*, *46*, 3975–3986.

Li, Q., and W. S. Kiefer (2007), Mantle convection and magma production on present-day Mars: Effects of temperature-dependent rheology, *Geophys. Res. Lett.*, *34*, L16203, doi:10.1029/2007GL030544.

MacKinnon, D. J., and K. L. Tanaka (1989), The impacted Martian crust: Structure, hydrology, and some geologic implications, *J. Geophys. Res.*, *94*, 17,359–17,370, doi:10.1029/JB094iB12p17359.

Manga, M. (2004), Martian floods at Cerberus Fossae can be produced by groundwater discharge, *Geophys. Res. Lett.*, *31*, L02702, doi:10.1029/2003GL018958.

Mangold, N., C. Quantin, V. Ansan, C. Delacourt, and P. Allemand (2004), Evidence for precipitation on Mars from Dendritic valleys in the Valles Marineris area, *Science*, *305*, 78–81, doi:10.1126/science.1097549.

Manning, C. E., and S. E. Ingebritsen (1999), Permeability of the continental crust: Implications of geothermal data and metamorphic systems, *Rev. Geophys.*, *37*, 127–150, doi:10.1029/1998RG900002.

Max, M. D., and S. M. Clifford (2000), The state, potential distribution, and biological implications of methane in the Martian crust, *J. Geophys. Res.*, *105*, 4165–4171, doi:10.1029/1999JE001119.

Max, M. D., and W. P. Dillon (1998), Oceanic methane hydrate: The character of the Blake Ridge hydrate stability zone, and the potential for methane extraction, *J. Pet. Geol.*, *21*, 343–358, doi:10.1111/j.1747-5457.1998.tb00786.x.

McGovern, P. J., S. C. Solomon, D. E. Smith, M. T. Zuber, M. Simons, M. A. Wieczorek, R. J. Phillips, G. A. Neumann, O. Aharonson, and J. W. Head (2004), Correction to "Localized gravity/topography admittance and correlation spectra on Mars: Implications for regional and global evolution," *J. Geophys. Res.*, *109*, E07007, doi:10.1029/2004JE002286.

Mellon, M. T., and B. M. Jakosky (1993), Geographic variations in the thermal and diffusive stability of ground ice on Mars, *J. Geophys. Res.*, *98*, 3345–3364, doi:10.1029/92JE02355.

Mellon, M. T., and B. M. Jakosky (1995), The distribution and behavior of Martian ground ice during past and present epochs, *J. Geophys. Res.*, *100*(E6), 11,781–11,799, doi:10.1029/95JE01027.

Mellon, M. T., B. M. Jakosky, and S. E. Postawko (1997), The persistence of equatorial ground ice on Mars, *J. Geophys. Res.*, *102*, 19,357–19,369, doi:10.1029/97JE01346.

Melosh, H. J., and A. M. Vickery (1989), Impact erosion of the primordial atmosphere of Mars, *Nature*, *338*, 487–489, doi:10.1038/338487a0.

Miller, G. C., V. Lepak, R. Kempley, and J. Awadh (2006), Photooxidation of chloride to perchlorate in the presence of desert soils and titanium dioxide, paper presented at 231st National Meeting, Am. Chem. Soc. Atlanta, 26–30 Mar.

Mitrofanov, I., et al. (2002), Maps of subsurface hydrogen from the high energy neutron detector, Mars Odyssey, *Science*, *297*, 78–81, doi:10.1126/science.1073616.

Mumma, M. J., R. E. Novak, M. A. DiSanti, B. P. Bonev, and N. Dello Russo (2004), Detection and mapping of methane and water on Mars, *Bull. Am. Astron. Soc.*, *36*, 1127.

Mumma, M. J., L. G. L. Villanueva, R. E. Novak, T. Hewagama, B. P. Bonev, M. A. DiSanti, A. M. Mandell, and M. D. Smith (2009), Strong release of methane on Mars in northern summer, *Science*, *323*, 1041–1045, doi:10.1126/science.1165243.

Nimmo, F., and K. Tanaka (2005), Early crustal evolution of Mars, *Annu. Rev. Earth Planet. Sci.*, *33*, 133–161, doi:10.1146/annurev.earth.33.092203.122637.

Onstott, T. C., D. McGown, J. Kessler, B. Sherwood Lollar, K. K. Lehmann, and S. M. Clifford (2006), Martian CH_4: Sources, flux, and detection, *Astrobiology*, *6*, 377–395, doi:10.1089/ast.2006.6.377.

Oyama, V. I., and B. J. Berdahl (1977), The Viking gas exchange experiment results from Chryse and Utopia surface samples, *J. Geophys. Res.*, *82*, 4669–4676, doi:10.1029/JS082i028p04669.

Phillips, R. J., et al. (2008), Mars north polar deposits: Stratigraphy, age, and geodynamical response, *Science*, *320*, 1182–1185, doi:10.1126/science.1157546.

Picardi, G., et al. (2003), Mars Advanced Radar for Subsurface and Ionosphere Sounding (MARSIS): Subsurface performances evaluation, in *2003 Proceedings of the International Conference on Radar*, pp. 515–521, doi:10.1109/RADAR.2003.1278795, Inst. of Electr. and Electr. Eng., Piscataway, N. J.

Picardi, G., et al. (2004), Performance and surface scattering models for the Mars Advanced Radar for Subsurface and Ionosphere Sounding (MARSIS), *Planet. Space Sci.*, *52*, 149–156, doi:10.1016/j.pss.2003.08.020.

Plaut, J. J., et al. (2007), Subsurface radar sounding of the south polar layered deposits of Mars, *Science*, *316*, 92–95, doi:10.1126/science.1139672.

Pollack, H. N., S. J. Hurter, and J. R. Johnson (1993), Heat flow from the Earth's interior—Analysis of the global data set, *Rev. Geophys.*, *31*, 267–280, doi:10.1029/93RG01249.

Presley, M. A., and P. R. Christensen (1997), The effect of bulk density and particle size sorting on the thermal conductivity of particulate materials under Martian atmospheric pressures, *J. Geophys. Res.*, *102*, 9221–9229, doi:10.1029/97JE00271.

Robertson, E. C., and D. L. Peck (1974), Thermal conductivity of vesicular basalt from Hawaii, *J. Geophys. Res.*, *79*, 4875–4888, doi:10.1029/JB079i032p04875.

Romig, P. R., B. D. Rodriguez, and M. H. Powers (1983), Geophysical methodology studies for military groundwater exploration, *Rep. AD-A137816*, 84 pp., U.S. Army Mobility Equip. Res. and Dev. Command, Fort Belvoir, Va.

Rossbacher, L. A., and S. Judson (1981), Ground ice on Mars: Inventory, distribution, and resulting landforms, *Icarus*, *45*, 39–59, doi:10.1016/0019-1035(81)90005-1.

Schorghofer, N. (2008), Temperature response of Mars to Milankovitch cycles, *Geophys. Res. Lett.*, *35*, L18201, doi:10.1029/2008GL034954.

Schorghofer, N., and O. Aharonson (2005), Stability and exchange of subsurface ice on Mars, *J. Geophys. Res.*, *110*, E05003, doi:10.1029/2004JE002350.

Segura, T. I., O. B. Toon, A. Colaprete, and K. Zahnle (2002), Environmental effects of large impacts on Mars, *Science*, *298*(5600), 1977–1980, doi:10.1126/science.1073586.

Sloan, E. D., Jr. (1997), *Clathrate Hydrates of Natural Gases*, Marcel Dekker, New York.

Smith, D., G. Neumann, R. E. Arvidson, E. A. Guinness, and S. Slavney (2003), Mars Global Surveyor Laser Altimeter Mission Experiment Gridded Data Record, http://starbrite.jpl.nasa.gov/pds/viewDataset.jsp?dsid = MGS-M-MOLA-5-MEGDR-L3-V1.0, NASA Planet. Data Syst., Greenbelt, Md.

Solomon, S. C., and J. W. Head (1990), Heterogeneities in the thickness of the elastic lithosphere of Mars: Constraints on heat flow and internal dynamics, *J. Geophys. Res.*, *95*, 11,073–11,083, doi:10.1029/JB095iB07p11073.

Solomon, S. C., et al. (2005), New perspectives on ancient Mars, *Science*, *307*, 1214–1220, doi:10.1126/science.1101812.

Tanaka, K. L. (1986), The stratigraphy of Mars, *J. Geophys. Res.*, *91*, E139–E158, doi:10.1029/JB091iB13p0E139.

Tittmann, B. R. (1979), Brief note for consideration of active seismic exploration on Mars, *J. Geophys. Res.*, *84*, 7940–7942, doi:10.1029/JB084iB14p07940.

Tosca, N. J. A. H. K., and S. M. McLennanet (2008), Water activity and the challenge for life on early Mars, *Science*, *320*, 1204–1207, doi:10.1126/science.1155432.

Touma, J., and J. Wisdom (1993), The chaotic obliquity of Mars, *Science*, *259*, 1294–1296, doi:10.1126/science.259.5099.1294.

Travis, B. J., and W. C. Feldman (2009), Salt deposits, ice lenses and convective brine aquifers on Mars, *Lunar Planet. Sci.*, *XXXX*, abstract 1315.

Travis, B. J., N. D. Rosenberg, and J. N. Cuzzi (2003), On the role of widespread subsurface convection in bringing liquid water close to Mars' surface, *J. Geophys. Res.*, *108*(E4), 8040, doi:10.1029/2002JE001877.

Valeille, A., S. W. Bougher, V. Tenishev, M. R. Combi, and A. F. Nagy (2010), Water loss and evolution of the upper atmosphere and exosphere over Martian history, *Icarus*, *206*, 28–39, doi:10.1016/j.icarus.2009.04.036.

Ward, W. R. (1974), Climatic variations on Mars: 1. Astronomical theory of insolation, *J. Geophys. Res.*, *79*, 3375–3386, doi:10.1029/JC079i024p03375.

Ward, W. R. (1992), Long-term orbital and spin dynamics of Mars, in *Mars*, edited by H. H. Kieffer et al., pp. 298–320, Univ. of Ariz. Press, Tuscon, Ariz.

Watters, T. R., P. J. McGovern, and R. P. Irwin III (2007a), Hemispheres apart: The crustal dichotomy on Mars, *Annu. Rev. Earth Planet. Sci.*, *35*, 621–652, doi:10.1146/annurev.earth.35.031306.140220.

Watters, T. R., et al. (2007b), Radar sounding of the Medusae Fossae formation Mars: Equatorial ice or dry, low-density deposits?, *Science*, *318*, 1125–1128, doi:10.1126/science.1148112.

White, O. L., et al. (2009), MARSIS radar sounder observations in the vicinity of Ma'adim Vallis, Mars, *Icarus*, *201*, 460–473, doi:10.1016/j.icarus.2009.01.015.

Wood, S. E., and S. D. Griffiths (2009), Mars subsurface warming due to atmospheric collapse at low obliquity, *Lunar Planet. Sci.*, *XXXX*, abstract 2490.

Zent, A. P., F. P. Fanale, J. R. Salvail, and S. E. Postawko (1986), Distribution and state of H_2O in the high-latitude shallow subsurface of Mars, *Icarus*, *67*, 19–36, doi:10.1016/0019-1035(86)90171-5.

J. Boisson and E. Heggy, Equipe Géophysique Spatiale et Planétaire, Institut de Physique du Globe de Paris, Université Paris Diderot, CNRS, 4 Ave. de Neptune, F-94107 St Maur des Fosses, France.

S. M. Clifford, J. Lasue, and P. McGovern, Lunar and Planetary Institute, 3600 Bay Area Blvd., Houston, TX 77058, USA. (clifford@lpi.usra.edu)

M. D. Max, MDS Research, 1601 3rd St. S, St. Petersburg, FL 33701-5552, USA.